

Aligning Theory with Practice for Muon-type Optimizers: A Layer-wise Framework

Artem Riabinin

ARTEM.RIABININ@KAUST.EDU.SA

Egor Shulgin

SHULGIN.YEGOR@GMAIL.COM

Kaja Gruntkowska

KAJA.GRUNTKOWSKA@KAUST.EDU.SA

Peter Richtárik

PETER.RICHTARIK@KAUST.EDU.SA

King Abdullah University of Science and Technology (KAUST), Saudi Arabia

Abstract

Recent developments in deep learning optimization have brought about radically new algorithms based on the Linear Minimization Oracle (LMO) framework, such as **Muon** [16] and **Scion** [29]. After over a decade of **Adam**’s dominance, these LMO-based methods are emerging as viable replacements, offering several practical advantages such as improved memory efficiency, better hyperparameter transferability, and most importantly, superior empirical performance on large-scale tasks, including LLM training. However, a significant gap remains between their practical use and our current theoretical understanding: prior analyses (1) overlook the layer-wise LMO application of these optimizers in practice, and (2) rely on an unrealistic smoothness assumption, leading to impractically small stepsizes. To address both, we propose a new LMO-based method called **Gluon**, capturing prior theoretically analyzed methods as special cases, and introduce a new refined generalized smoothness model that captures the layer-wise geometry of neural networks, matches the layer-wise practical implementation of **Muon** and **Scion**, and leads to convergence guarantees with strong practical predictive power. Unlike prior results, our theoretical stepsizes closely match the fine-tuned values reported by Pethick et al. [29]. Our experiments with NanoGPT and CNN confirm that our assumption holds along the optimization trajectory, ultimately closing the gap between theory and practice.

1. Introduction

The success of deep learning models across a wide range of challenging domains is inseparable from the optimization algorithms used to train them. As neural networks have grown deeper and datasets larger, optimization has quietly become one of the most consequential components of modern machine learning (ML). Nowhere is this more evident than in the training of large language models (LLMs), which routinely consume thousands of GPU-hours. **Adam** [19] (and lately **AdamW** [26])—being effective, relatively reliable, and widely adopted—has for over a decade served as the default choice for this task. While this reliance has powered much of deep learning’s progress, it has also exposed the shortcomings of adaptive moment estimation as a one-size-fits-all solution—namely, sensitivity to learning rate schedules, heavy tuning requirements [34], and poor generalization when not carefully calibrated [38]. However, a shift may now be underway. Recent optimizers, such as **Muon** [16] and **Scion** [29], represent a significant departure from **Adam**-type methods: they forgo the adaptive moment estimation in favor of a geometry-aware approach inspired by Frank-Wolfe

algorithms [8, 30]. These optimizers are not only simpler to implement and easier to tune, but also appear empirically stronger, outperforming `AdamW` in LLM training [24, 29].

Yet, despite their potential, these new methods are still in their infancy, and our understanding of their theoretical foundations and practical utility in LLM training remains incomplete. Prior convergence guarantees in realistic nonconvex regimes are still far from satisfactory. Indeed, as we argue in 2, the (very few) existing theoretical analyses *fail to capture the true algorithms used in practice*, focusing instead on simplified variants that diverge from actual implementations. We identify two key mismatches—*neglect of layer-wise structure* (2.1) and flawed stepsize choices stemming from an *inaccurate smoothness model* (2.2)—and close this gap with a *solution to both*. We elaborate on these advances in the remainder of the paper.

To this end, we introduce `Gluon`, a unified framework that faithfully models the layer-wise nature of modern LMO-based optimizers. Our core technical contribution is a novel **layer-wise** (L^0, L^1)-**smoothness** assumption (1) that offers a more realistic model of the loss landscapes in deep learning than classical smoothness. Building on this new assumption, we provide the first principled convergence analysis for this class of algorithms (1), yielding adaptive, layer-wise stepsizes and sharper theoretical guarantees. Finally, we provide extensive empirical evidence (4) confirming that our assumption holds in practice and that our theory provides a sound basis for understanding and designing these optimizers. A detailed breakdown of these contributions can be found in B.

Our goal is to solve the general optimization problem $\min_{X \in \mathcal{S}} \{f(X) := \mathbb{E}_{\xi \sim \mathcal{D}} [f_\xi(X)]\}$, where \mathcal{S} is a finite-dimensional vector space and $f_\xi : \mathcal{S} \mapsto \mathbb{R}$ are potentially non-convex and non-smooth but continuously differentiable functions. Here, $f_\xi(X)$ represents the loss of model parameterized by X associated with training data point ξ sampled from probability distribution \mathcal{D} . To make the problem meaningful, we assume that $f^{\inf} \stackrel{\text{def}}{=} \inf_{X \in \mathcal{S}} f(X) > -\infty$. In this work we are particularly interested in the scenario when the parameter vector $X \in \mathcal{S}$ is obtained by collecting the matrices $X_i \in \mathcal{S}_i \stackrel{\text{def}}{=} \mathbb{R}^{m_i \times n_i}$ of trainable parameters across all layers $i = 1, \dots, p$ of a deep model. For simplicity, we therefore write $X = [X_1, \dots, X_p]$. This means that, formally, \mathcal{S} is the d -dimensional product space $\mathcal{S} \stackrel{\text{def}}{=} \bigotimes_{i=1}^p \mathcal{S}_i \equiv \mathcal{S}_1 \otimes \dots \otimes \mathcal{S}_p$, where $d \stackrel{\text{def}}{=} \sum_{i=1}^p m_i n_i$. With each space \mathcal{S}_i we associate the trace inner product $\langle X_i, Y_i \rangle_{(i)} \stackrel{\text{def}}{=} \text{tr}(X_i^\top Y_i)$ for $X_i, Y_i \in \mathcal{S}_i$, and an arbitrary norm $\|\cdot\|_{(i)}$, not necessarily induced by the inner product.

2. Theory vs. practice of Muon and Scion

In this work, we focus on an algorithm based on iteratively calling linear minimization oracles (LMOs) across all layers, formalized in 2, for which we coin the name `Gluon`. In particular, for each layer i , independently across all layers, `Gluon` iteratively updates the parameters via

$$X_i^{k+1} = \text{LMO}_{\mathcal{B}_i^k} \left(M_i^k \right) \stackrel{\text{def}}{=} \arg \min_{X_i \in \mathcal{B}_i^k} \langle M_i^k, X_i \rangle_{(i)}, \text{ where } \mathcal{B}_i^k \stackrel{\text{def}}{=} \{X_i \in \mathcal{S}_i : \|X_i - X_i^k\|_{(i)} \leq t_i^k\},$$

where $t_i^k > 0$ is an adaptively chosen stepsize/radius/learning rate.¹ Note that the momentum $M^k = [M_1^k, \dots, M_p^k] \in \mathcal{S}$ accumulates the contributions from the stochastic gradients $\nabla f_{\xi^k}(X^k) = [\nabla_1 f_{\xi^k}(X^k), \dots, \nabla_p f_{\xi^k}(X^k)] \in \mathcal{S}$ (see Step 2 of 2).

1. In this context, the radii defining the norm balls in the LMOs effectively act as stepsizes—see D.1. Accordingly, we use the terms *radius*, *stepsize*, and *learning rate* interchangeably throughout.

The [Gluon](#) framework generalizes a range of methods, including [Muon](#) and [Scion](#), which are recovered as special cases under specific norm choices (see 3.1 and E.1). Beyond their ability to outperform [AdamW](#) on large-scale benchmarks, these optimizers offer a number of attractive properties: improved memory efficiency, greater robustness to hyperparameter settings, and the ability to transfer those settings across model sizes [29, 32]. Moreover, in contrast to [Adam](#), they were theoretically analyzed shortly after release and are guaranteed to converge under standard assumptions of Lipschitz smoothness² and bounded variance of stochastic gradients [20, 22, 29].

[Gluon](#) presents the method that is deployed in practice [15, 28] and has proven highly effective. That said, we argue that existing analyses [20, 22, 29] do *not* accurately reflect this implementation, diverging from it in two key ways. As such, they *fail to explain why the algorithm performs so well*. Let us detail why.

2.1. Layer-wise structure

First, we briefly walk through the theoretical understanding offered by previous studies. [Muon](#) is an optimizer specifically designed for hidden layers, leaving the first and last layers to be handled by some other optimizer, e.g., [Adam\(W\)](#). Its original introduction by Jordan et al. [16] was purely empirical, with no attempt at theoretical analysis. The first convergence result came from Li and Hong [22], who analyzed the smooth nonconvex setting but focused solely on problem with $p = 1$, effectively limiting the scope to the single-layer case. The [Scion](#)³ optimizer (a special case of [Gluon](#)) proposed by Pethick et al. [29] improves upon [Muon](#) by applying the LMO-based rule to all layers, ultimately achieving better empirical performance. Both this work and that of Kovalev [20] analyze (a variant of) the general update rule

$$M^k = \beta^k M^{k-1} + (1 - \beta^k) \nabla f_{\xi^k}(X^k), \quad X^{k+1} = \text{LMO}_{\mathcal{B}^k}(M^k), \quad (1)$$

where $\beta^k \in [0, 1)$ is momentum, $\nabla f_{\xi^k}(X^k)$ is the stochastic gradient sampled at iteration k , and $\mathcal{B}^k \stackrel{\text{def}}{=} \{X \in \mathcal{S} : \|X - X^k\| \leq t^k\}$ is a norm ball centered at X^k with stepsize $t^k > 0$. This setup closely resembles the structure of [Gluon](#), but is *not* exactly the same. Indeed, [Gluon](#) updates the parameters *layer-wise*, not jointly over the full vector X . This distinction is critical since for practical, extremely high-dimensional models, calculating a single global LMO for the entire parameter vector is prohibitively expensive, while breaking the problem into “smaller”, per-layer LMOs restores computational feasibility.

Motivated by this disconnect, we formulate our analysis in the matrix product space \mathcal{S} , explicitly honoring the layer-wise structure. This enables us to study the actual per-layer updates (18), with assumptions and hyperparameters adapted to each layer.

2.2. A theory with predictive power

All prior works claiming to guarantee convergence of 2 come with several serious analytical shortcomings—and these directly translate into practical deficiencies. Concretely, all existing analyses

2. A function $f : \mathcal{S} \mapsto \mathbb{R}$ is L -smooth if $\|\nabla f(x) - \nabla f(y)\|_* \leq L \|x - y\|$ for all $x, y \in \mathcal{S}$, where \mathcal{S} is a finite-dimensional vector space equipped with a norm $\|\cdot\|$ and $\|\cdot\|_*$ is the dual norm associated with $\|\cdot\|$.
3. Pethick et al. [29] introduce two variants of the [Scion](#) optimizer: one for constrained optimization, called simply “[Scion](#)”, and another for unconstrained problems, referred to as “[unScion](#)”. In this work, “[Scion](#)” refers to either variant, and “[unScion](#)” is used when referring to the unconstrained version.

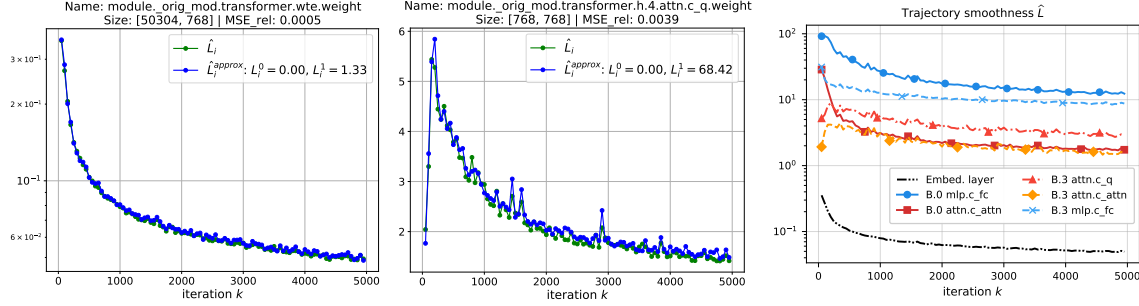


Figure 1: Token embedding matrix from the first/last layer. Figure 2: Self-attention query matrix from the 4th block. Figure 3: Trajectory smoothness across blocks (B.i) and layers.

Figure 4: Training NanoGPT on FineWeb validates our layer-wise (L^0, L^1) -smoothness model.

of Muon/Scion are built on the classical L -smoothness assumption, imposing a uniform smoothness constant across all layers. This is problematic, as *different layers have different geometries*, and thus *should be treated differently*.

But the issue runs much deeper. These algorithms are built for deep learning, where the objective functions are already well known *not* to be smooth [6, 37]. This mismatch has consequences: prior convergence analyses prescribe *tiny constant stepsizes* (see 1), uniform across all parameter groups, which bear little resemblance to the tuned learning rates that yield state-of-the-art empirical performance in practice. Consequently, they completely fail to explain why these methods perform so well empirically. In other words, the theory falls short at the one thing it should do best: guiding practical choices, leaving practitioners reliant on costly manual tuning.

Our result in 1 shows this mismatch is *not* inevitable. To better reflect the behavior of deep models, we introduce a more expressive regularity condition: the *layer-wise* (L_0, L_1) -smoothness⁴ –an extension of the generalized smoothness model of Zhang et al. [37], applied at the layer level.

Assumption 1 (Layer-wise (L^0, L^1) -smoothness) *The function $f : \mathcal{S} \mapsto \mathbb{R}$ is layer-wise (L_0, L_1) -smooth with constants $L^0 \stackrel{\text{def}}{=} (L_1^0, \dots, L_p^0) \in \mathbb{R}_+^p$ and $L^1 \stackrel{\text{def}}{=} (L_1^1, \dots, L_p^1) \in \mathbb{R}_+^p$. That is, the inequality*

$$\|\nabla_i f(X) - \nabla_i f(Y)\|_{(i)\star} \leq (L_i^0 + L_i^1 \|\nabla_i f(X)\|_{(i)\star}) \|X_i - Y_i\|_{(i)} \quad (2)$$

holds for all $i = 1, \dots, p$ and all $X = [X_1, \dots, X_p] \in \mathcal{S}$, $Y = [Y_1, \dots, Y_p] \in \mathcal{S}$, where $\|\cdot\|_{(i)\star}$ is the dual norm associated with $\|\cdot\|_{(i)}$ (i.e., $\|X_i\|_{(i)\star} \stackrel{\text{def}}{=} \sup_{\|Z_i\|_{(i)} \leq 1} \langle X_i, Z_i \rangle_{(i)}$ for any $X_i \in \mathcal{S}_i$).

Assumption 1 can be viewed as a generalization of the anisotropic “vector” (L^0, L^1) -smoothness introduced by Liu et al. [25] (now framed in terms of arbitrary norms), which itself is a generalization of the (L^0, L^1) -smoothness model of Zhang et al. [37]. As such, our analysis of Gluon goes beyond all existing results, which have only considered the classical L -smooth setting. Crucially, however,

4. While we state 1 in this general form, it is worth noting that the proofs do not rely on its full strength. In all cases, we only require the assumption to hold for pairs X, Y such that $\|X - Y\| < c$ for some constant $c \geq 0$ (where $\|\cdot\|$ is any norm on \mathcal{S}). Specifically, the assumption is only invoked with $X = X^k, Y = X^{k+1}$, and since the stepsizes we use are bounded, the distances between consecutive iterates remain bounded as well.

this is *not* generalization for its own sake—we argue that this is in fact *the right* model for the problem setting at hand. Why? There are (at least) two reasons.

First, unlike classical L -smoothness, our formulation *aligns very closely with empirical observations*. In Figures 1 and 2, we validate Assumption 1 in the context of training NanoGPT on the FineWeb dataset. We plot estimated *trajectory smoothness* $\hat{L}_i[k] \stackrel{\text{def}}{=} \|\nabla_i f_{\xi^{k+1}}(X^{k+1}) - \nabla_i f_{\xi^k}(X^k)\|_{(i)*}/\|X_i^{k+1} - X_i^k\|_{(i)}$ alongside the approximation $\hat{L}_i^{\text{approx}}[k] \stackrel{\text{def}}{=} L_i^0 + L_i^1 \|\nabla_i f_{\xi^{k+1}}(X^{k+1})\|_{(i)*}$, where L_i^0, L_i^1 are layer-specific parameters estimated from the training run. The figures show these quantities for parameters from the embedding layer and one of the transformer blocks. The close correspondence between $\hat{L}_i[k]$ and $\hat{L}_i^{\text{approx}}[k]$ provides strong evidence that Assumption 1 holds approximately along the training trajectory. In G, we further corroborate this finding, showing that our assumption is satisfied *across the entire model architecture* for both the NanoGPT language modeling task and a CNN trained on CIFAR-10. In all cases, we find that $L_i^0 \approx 0$ for all i , again highlighting the limitations of classical smoothness. Moreover, as shown in 3, trajectory smoothness varies substantially across blocks and layers, underscoring the need for per-layer treatment. Together, these results suggest that layer-wise (L^0, L^1) -smoothness offers a *significantly more realistic model of the loss landscape in modern deep learning*.

Secondly, 1 not only better captures the geometry of the models, but also *directly informs the design of adaptive and practically effective stepsizes*. In 1, we derive learning rates that reflect the local geometry of each parameter group, guided by our layer-wise smoothness model. As demonstrated in 4, our theoretically grounded stepsizes turn out to be *almost the same as the ones obtained by Pethick et al. [29] via hyperparameter tuning*—a striking validation of our approach, which further highlights the need for layer-wise reasoning.

3. Main theory and results

To gain a better intuition into the structure of the updates, we begin with a deterministic formulation of Gluon, formalized in Algorithm 1. At each iteration, the method independently minimizes a linear approximation of f around each parameter group X_i^k within a ball of radius $t_i^k > 0$, ultimately allowing for layer-specific algorithmic design choices.

3.1. Examples of optimizers satisfying our framework

Deterministic Gluon describes a general class of methods, parameterized by the choice of norms $\|\cdot\|_{(i)}$ in the LMO. To illustrate the flexibility of this framework, we highlight several notable special cases (see E.1 for more details). First, observe that the update rule (7) can be written as

$$X_i^{k+1} = X_i^k + t_i^k \text{LMO}_{\{X_i \in \mathcal{S}_i : \|X_i\|_{(i)} \leq 1\}} \left(\nabla_i f(X^k) \right) = X_i^k + t_i^k \underset{\|X_i\|_{(i)} \leq 1}{\operatorname{argmin}} \langle \nabla_i f(X^k), X_i \rangle_{(i)}. \quad (3)$$

For any $X_i \in \mathcal{S}_i = \mathbb{R}^{m_i \times n_i}$, define $\|X_i\|_{\alpha \rightarrow \beta} \stackrel{\text{def}}{=} \sup_{\|z\|_\alpha=1} \|X_i z\|_\beta$, where $\|\cdot\|_\alpha$ and $\|\cdot\|_\beta$ are some (possibly non-Euclidean) norms on \mathbb{R}^{n_i} and \mathbb{R}^{m_i} , respectively. Note that (3) naturally recovers several known updates for specific choices of the layer norms, e.g., layer-wise normalized GD [36] for Euclidean norms $\|\cdot\|_{(i)} = \|\cdot\|_2$, and layer-wise signGD [1] for max-norms $\|\cdot\|_{(i)} = \|\cdot\|_\infty$.

Two special cases are particularly relevant to our analysis: Muon and the unScion optimizer for LLM training. Their specific update rules, which are recovered by our framework, are detailed in E.1.

Having demonstrated the framework’s flexibility through concrete examples, we now state a general convergence result for deterministic **Gluon**.

Theorem 1 *Let 1 hold and fix $\varepsilon > 0$. Let X^0, \dots, X^{K-1} be the iterates of deterministic **Gluon** (Algorithm 1) run with stepsizes $t_i^k = \frac{\|\nabla_i f(X^k)\|_{(i)\star}}{L_i^0 + L_i^1 \|\nabla_i f(X^k)\|_{(i)\star}}$. Then, to guarantee that*

$$\min_{k=0, \dots, K-1} \sum_{i=1}^p \frac{1/L_i^1}{\frac{1}{p} \sum_{j=1}^p 1/L_j^1} \|\nabla_i f(X^k)\|_{(i)\star} \leq \varepsilon, \quad (4)$$

it suffices to run the algorithm for

$$K = \left\lceil \frac{2\Delta^0 (\sum_{i=1}^p L_i^0 / (L_i^1)^2)}{\varepsilon^2 \left(\frac{1}{p} \sum_{j=1}^p 1/L_j^1 \right)^2} + \frac{2\Delta^0}{\varepsilon \left(\frac{1}{p} \sum_{j=1}^p 1/L_j^1 \right)} \right\rceil \quad (5)$$

iterations, where $\Delta^0 \stackrel{\text{def}}{=} f(X^0) - f^{\text{inf}}$.

When $p = 1$, our rates match the best-known complexity for finding a stationary point of (L^0, L^1) -smooth functions, $\mathcal{O}(L^0 \Delta^0 / \varepsilon^2 + L^1 \Delta^0 / \varepsilon)$, as established by Vankov et al. [33] for the Gradient Method. While no prior work has analyzed deterministic **Gluon** under general (L^0, L^1) -smoothness, there exist analyses under classical L -smoothness, treating the parameters as a single vector. The analysis by Kovalev [20] guarantees convergence in $K = \lceil 6L\Delta^0 / \varepsilon^2 \rceil$ iterations. The same bound appears in Li and Hong [22] and Pethick et al. [29] (by setting $\sigma^2 = 0$). Since for $p = 1$, L -smoothness implies 1 with $L^1 = 0$ (3), our rates match these prior results up to a constant factor. Thus, even in the smooth setting, our bounds are as tight as those derived specifically for it.

However, the real strength of our guarantees lies in their broader applicability. Our analysis is much more general than prior studies, as it extends beyond standard smoothness—allowing $L_i^1 > 0$ introduces additional terms that drive the accelerated convergence enabled by (L^0, L^1) -smoothness. This richer model is *essential for explaining the empirical speedup* of methods like **Muon**, and much more accurately reflects the geometry of neural network loss surfaces. Indeed, as we demonstrate in 4, the assumption typically holds with $L_i^0 \approx 0$ and $L_i^1 > 0$.

Practical radii t_i^k . Unlike previous analyses [20, 22, 29], which prescribe impractically small constant radii proportional to ε , our framework allows t_i^k to be *adaptive* to the loss landscape. Therefore, t_i^k can be larger early in training when $\|\nabla_i f(X^k)\|_{(i)\star}$ is large and gradually shrink as the gradient norm decreases. In the special case when $L_i^0 \approx 0$ (as observed empirically), $t_i^k \approx 1/L_i^1$, which is substantially larger than the radii dictated by earlier analyses. Crucially, as shown in 4, our adaptive stepsizes closely match those that yield state-of-the-art empirical performance identified by Pethick et al. [29] through hyperparameter tuning.

4. Experiments

We conduct experiments to validate our central claim: that layer-wise (L^0, L^1) -smoothness (1) is a realistic and useful model for modern deep learning optimizers. To this end, we train a 124M parameter NanoGPT model on the FineWeb dataset using the **unScion** optimizer. Our central finding, illustrated in 4, is that the (L^0, L^1) -smoothness model accurately captures the empirical

trajectory smoothness across different layers of the transformer, whereas classical L -smoothness does not.

This result has direct practical implications. Based on the fitted smoothness parameters from the training run, our theory suggests layer-specific stepsizes of approximately $t_i^k \approx 1/70 \approx 0.014$ for transformer block layers and a much larger $t_p^k \approx 1/1.3 \approx 0.77$ for the embedding and output layers. This theoretically-derived structural difference justifies the empirical discovery that using significantly different learning rates for these groups is critical for state-of-the-art performance. Thus, our framework provides a principled foundation for guiding hyperparameter design. All detailed experimental procedures, additional figures, and further ablation studies—including a validation on CNNs—are provided in G.

Acknowledgements

The research reported in this publication was supported by funding from King Abdullah University of Science and Technology (KAUST): i) KAUST Baseline Research Scheme, ii) CRG Grant ORFS-CRG12-2024-6460, iii) Center of Excellence for Generative AI, under award number 5940, and iv) SDAIA-KAUST Center of Excellence in Artificial Intelligence and Data Science.

References

- [1] Lukas Balles, Fabian Pedregosa, and Nicolas Le Roux. The geometry of Sign Gradient Descent, 2020. URL <https://arxiv.org/abs/2002.08056>. (Cited on page 5 and 18)
- [2] Jeremy Bernstein and Laker Newhouse. Modular duality in deep learning. *arXiv preprint arXiv:2410.21265*, 2024. URL <https://arxiv.org/abs/2410.21265>. (Cited on page 16)
- [3] Jeremy Bernstein and Laker Newhouse. Old optimizer, new norm: An anthology. In *OPT 2024: Optimization for Machine Learning*, 2024. URL <https://arxiv.org/abs/2409.20325>. (Cited on page 12 and 18)
- [4] Jeremy Bernstein, Yu-Xiang Wang, Kamyar Azizzadenesheli, and Animashree Anandkumar. signSGD: Compressed optimisation for non-convex problems. In *International Conference on Machine Learning*, pages 560–569. PMLR, 2018. URL <https://arxiv.org/abs/1802.04434>. (Cited on page 12)
- [5] Aleksandr Beznosikov, Samuel Horváth, Peter Richtárik, and Mher Safaryan. On biased compression for distributed learning. *Journal of Machine Learning Research*, 24(276):1–50, 2023. (Cited on page 27)
- [6] Michael Crawshaw, Mingrui Liu, Francesco Orabona, Wei Zhang, and Zhenxun Zhuang. Robustness to unbounded smoothness of generalized signSGD. *Advances in neural information processing systems*, 35:9955–9968, 2022. URL <https://arxiv.org/abs/2208.11195>. (Cited on page 4 and 12)
- [7] Yury Demidovich, Grigory Malinovsky, Igor Sokolov, and Peter Richtárik. A guide through the zoo of biased sgd. *Advances in Neural Information Processing Systems*, 36:23158–23171, 2023. (Cited on page 27)

- [8] Marguerite Frank and Philip Wolfe. An algorithm for quadratic programming. *Naval Research Logistics Quarterly*, 3(1-2):95–110, 1956. URL <https://onlinelibrary.wiley.com/doi/abs/10.1002/nav.3800030109>. (Cited on page 2 and 12)
- [9] Eduard Gorbunov, Nazarii Tupitsa, Sayantan Choudhury, Alen Aliev, Peter Richtárik, Samuel Horváth, and Martin Takáč. Methods for convex (L_0, L_1) -smooth optimization: Clipping, acceleration, and adaptivity. In *The Thirteenth International Conference on Learning Representations*, 2025. URL <https://arxiv.org/abs/2409.14989>. (Cited on page 12)
- [10] Kaja Gruntkowska, Hanmin Li, Aadi Rane, and Peter Richtárik. The Ball-Proximal ("Broximal") Point Method: a new algorithm, convergence theory, and applications. *arXiv preprint arXiv:2502.02002*, 2025. URL <https://arxiv.org/abs/2502.02002>. (Cited on page 16)
- [11] Florian Hübler, Junchi Yang, Xiang Li, and Niao He. Parameter-agnostic optimization under relaxed smoothness. In *International Conference on Artificial Intelligence and Statistics*, pages 4861–4869. PMLR, 2024. URL <https://arxiv.org/abs/2311.03252>. (Cited on page 12, 15, 26, and 34)
- [12] Martin Jaggi. Revisiting frank-wolfe: Projection-free sparse convex optimization. In *International conference on machine learning*, pages 427–435. PMLR, 2013. (Cited on page 12)
- [13] Ruichen Jiang, Devyani Maladkar, and Aryan Mokhtari. Convergence analysis of adaptive gradient methods under refined smoothness and noise assumptions. *arXiv preprint arXiv:2406.04592*, 2024. URL <https://arxiv.org/abs/2406.04592>. (Cited on page 12)
- [14] Keller Jordan. Cifar-10 airbench. <https://github.com/KellerJordan/cifar10-airbench>, 2024. GitHub repository. (Cited on page 39 and 43)
- [15] Keller Jordan, Jeremy Bernstein, Ben Rappazzo, B. Vlado, Y. Jiacheng, F. Cesista, and B. Koszarsky. Modded-nanoGPT: Speedrunning the nanoGPT baseline. <https://github.com/KellerJordan/modded-nanogpt>, 2024. GitHub repository. Additional contributors: @fern-bear.bsky.social, @Grad62304977. (Cited on page 3 and 39)
- [16] Keller Jordan, Yuchen Jin, Vlado Boza, Jiacheng You, Franz Cesista, Laker Newhouse, and Jeremy Bernstein. Muon: An optimizer for hidden layers in neural networks, 2024. URL <https://kellerjordan.github.io/posts/muon/>. (Cited on page 1, 3, 12, 18, and 39)
- [17] Hamed Karimi, Julie Nutini, and Mark Schmidt. Linear convergence of gradient and proximal-gradient methods under the Polyak-Łojasiewicz condition, 2020. URL <https://arxiv.org/abs/1608.04636>. (Cited on page 23)
- [18] Ahmed Khaled and Peter Richtárik. Better theory for SGD in the nonconvex world. *arXiv preprint arXiv:2002.03329*, 2020. URL <https://arxiv.org/abs/2002.03329>. (Cited on page 27 and 47)
- [19] Diederik P Kingma and Jimmy Ba. Adam: A method for stochastic optimization. In *International Conference on Learning Representations*, 2015. URL <https://arxiv.org/abs/1412.6980>. (Cited on page 1)

- [20] Dmitry Kovalev. Understanding gradient orthogonalization for deep learning via non-Euclidean trust-region optimization, 2025. URL <https://arxiv.org/abs/2503.12645>. (Cited on page 3, 6, 12, 16, and 17)
- [21] Tim Large, Yang Liu, Minyoung Huh, Hyojin Bahng, Phillip Isola, and Jeremy Bernstein. Scalable optimization in the modular norm. In *The Thirty-eighth Annual Conference on Neural Information Processing Systems*, 2024. URL <https://arxiv.org/abs/2405.14813>. (Cited on page 16)
- [22] Jiaxiang Li and Mingyi Hong. A note on the convergence of Muon and further, 2025. URL <https://arxiv.org/abs/2502.02900>. (Cited on page 3, 6, 12, and 17)
- [23] Chaoyue Liu, Libin Zhu, and Mikhail Belkin. Loss landscapes and optimization in over-parameterized non-linear systems and neural networks. *Applied and Computational Harmonic Analysis*, 59, 01 2022. doi: 10.1016/j.acha.2021.12.009. URL <https://arxiv.org/abs/2003.00307>. (Cited on page 23)
- [24] Jingyuan Liu, Jianlin Su, Xingcheng Yao, Zhejun Jiang, Guokun Lai, Yulun Du, Yidao Qin, Weixin Xu, Enzhe Lu, Junjie Yan, et al. Muon is scalable for LLM training. *arXiv preprint arXiv:2502.16982*, 2025. URL <https://arxiv.org/abs/2502.16982>. (Cited on page 2)
- [25] Yuxing Liu, Rui Pan, and Tong Zhang. AdaGrad under anisotropic smoothness, 2024. URL <https://arxiv.org/abs/2406.15244>. (Cited on page 4 and 12)
- [26] Ilya Loshchilov and Frank Hutter. Decoupled weight decay regularization. In *International Conference on Learning Representations*, 2019. URL <https://arxiv.org/abs/1711.05101>. (Cited on page 1)
- [27] Yu Nesterov. Efficiency of coordinate descent methods on huge-scale optimization problems. *SIAM Journal on Optimization*, 22(2):341–362, 2012. URL <https://pubs.siam.org/doi/10.1137/100802001>. (Cited on page 12)
- [28] Thomas Pethick, Wanyun Xie, Kimon Antonakopoulos, Zhenyu Zhu, Antonio Silveti-Falls, and Volkan Cevher. Scion. <https://github.com/LIONS-EPFL/scion.git>, 2025. GitHub repository. (Cited on page 3, 39, and 43)
- [29] Thomas Pethick, Wanyun Xie, Kimon Antonakopoulos, Zhenyu Zhu, Antonio Silveti-Falls, and Volkan Cevher. Training deep learning models with norm-constrained LMOs. *arXiv preprint arXiv:2502.07529*, 2025. URL <https://arxiv.org/abs/2502.07529>. (Cited on page 1, 2, 3, 5, 6, 12, 13, 16, 17, 18, 39, 42, and 44)
- [30] Sebastian Pokutta. The Frank-Wolfe algorithm: a short introduction. *Jahresbericht der Deutschen Mathematiker-Vereinigung*, 126(1):3–35, 2024. URL <https://arxiv.org/abs/2311.05313>. (Cited on page 2)
- [31] Peter Richtárik and Martin Takáč. Iteration complexity of randomized block-coordinate descent methods for minimizing a composite function. *Mathematical Programming*, 144(1):1–38, 2014. URL <https://arxiv.org/abs/1107.2848>. (Cited on page 12)

- [32] Ishaan Shah, Anthony M Polloreno, Karl Stratos, Philip Monk, Adarsh Chaluvaraju, Andrew Hojel, Andrew Ma, Anil Thomas, Ashish Tanwer, Darsh J Shah, et al. Practical efficiency of Muon for pretraining. *arXiv preprint arXiv:2505.02222*, 2025. URL <https://arxiv.org/abs/2505.02222>. (Cited on page 3)
- [33] Daniil Vankov, Anton Rodomanov, Angelia Nedich, Lalitha Sankar, and Sebastian U Stich. Optimizing (L_0, L_1) -smooth functions by gradient methods. In *The Thirteenth International Conference on Learning Representations*, 2025. URL <https://arxiv.org/abs/2410.10800>. (Cited on page 6, 12, and 18)
- [34] Ashia C Wilson, Rebecca Roelofs, Mitchell Stern, Nati Srebro, and Benjamin Recht. The marginal value of adaptive gradient methods in machine learning. *Advances in neural information processing systems*, 30, 2017. URL <https://arxiv.org/abs/1705.08292>. (Cited on page 1)
- [35] Shuo Xie, Mohamad Amin Mohamadi, and Zhiyuan Li. Adam exploits ℓ_∞ -geometry of loss landscape via coordinate-wise adaptivity. *arXiv preprint arXiv:2410.08198*, 2024. URL <https://arxiv.org/abs/2410.08198>. (Cited on page 12)
- [36] Adams Wei Yu, Lei Huang, Qihang Lin, Ruslan Salakhutdinov, and Jaime Carbonell. Block-normalized gradient method: An empirical study for training deep neural network, 2018. URL <https://openreview.net/forum?id=ry831QWAb>. (Cited on page 5 and 18)
- [37] Jingzhao Zhang, Tianxing He, Suvrit Sra, and Ali Jadbabaie. Why gradient clipping accelerates training: A theoretical justification for adaptivity. In *International Conference on Learning Representations*, 2020. URL <https://arxiv.org/abs/1905.11881>. (Cited on page 4, 12, and 13)
- [38] Difan Zou, Yuan Cao, Yuanzhi Li, and Quanquan Gu. Understanding the generalization of Adam in learning neural networks with proper regularization. *arXiv preprint arXiv:2108.11371*, 2021. URL <https://arxiv.org/abs/2108.11371>. (Cited on page 1)

Contents

1	Introduction	1
2	Theory vs. practice of Muon and Scion	2
2.1	Layer-wise structure	3
2.2	A theory with predictive power	3
3	Main theory and results	5
3.1	Examples of optimizers satisfying our framework	5
4	Experiments	6
A	Related works	12
B	Contributions	13
C	Auxiliary lemmas	14
D	Remarks on the theoretical results	16
D.1	Note on radii and stepsizes	16
D.2	Note on prior analyses	16
E	Deterministic case	17
E.1	Special cases of the LMO framework	17
E.2	Proof of Theorem 1	19
E.3	Convergence under the PŁ condition	23
F	Stochastic case	26
F.1	Adaptive stepsizes	27
F.2	Proof of Theorem 10	32
G	Additional experimental results and details	39
G.1	Experimental details	39
G.2	Fitting L_i^0 and L_i^1	39
G.3	Training NanoGPT on FineWeb.	39
G.3.1	Experimental Setup	39
G.3.2	Theoretical Stepsize Prediction	40
G.3.3	Empirical validation of 1	40
G.3.4	Generalized smoothness under Euclidean vs. specialized norms	41
G.3.5	Learning rate transfer from AdamW	42
G.3.6	Ablation Study on Learning Rate Scaling Factors	43
G.4	Training CNN on CIFAR-10	43
H	Conclusion and future work	47

Appendix A. Related works

Generalized Smoothness. The classical L -smoothness assumption, where the gradient is Lipschitz continuous with a global constant L , often fails to accurately capture the complex geometry of loss landscapes in deep learning [6, 37]. To address this, Zhang et al. [37] introduced the (L_0, L_1) -smoothness condition, empirically observing in language model experiments that a bound of the form $\|\nabla^2 f(x)\| \leq L_0 + L_1 \|\nabla f(x)\|$ better described the Hessian norm behavior. This model, where smoothness can depend on the gradient norm, allows for larger steps when gradients are small and more conservative steps when gradients are large, reflecting typical training dynamics. Subsequent works have analyzed standard optimization algorithms under this generalized smoothness framework. For instance, Gorbunov et al. [9] and Vankov et al. [33] provided convergence analyses for the Gradient Method. Hübner et al. [11] analyzed Normalized SGD with momentum in a parameter-agnostic setting under (L_0, L_1) -smoothness. Our work extends this line by incorporating (L_0, L_1) -smoothness into a *layer-wise* context using arbitrary norms, an approach that is particularly well-suited for the LMO-based optimizers we study.

Anisotropic Smoothness. Recognizing the heterogeneous nature of parameters in large models, researchers have explored anisotropic smoothness conditions, where smoothness constants can vary across different dimensions or parameter blocks. Early work in this direction includes coordinate-wise Lipschitz continuity for coordinate descent methods [27, 31]. More recently, Bernstein et al. [4] analyzed **signSGD** under a weaker notion of coordinate-wise smoothness. Crawshaw et al. [6] further developed this by analyzing Generalized **signSGD** under a generalized coordinate-wise smoothness assumption, highlighting that different parameter groups can exhibit vastly different geometries. Jiang et al. [13] focused on **Adagrad**’s analysis under coordinate-wise smoothness and established lower bounds for SGD, underscoring the benefits of adaptivity. Liu et al. [25] proposed “Anisotropic (L_0, L_1) -smoothness” (a vector version of (L_0, L_1) -smoothness applied coordinate-wise) and demonstrated **Adagrad**’s provable advantages over **SGD** in this setting. Xie et al. [35] also leveraged anisotropic smoothness concepts in their convergence analysis of **Adam**. Our work contributes by defining and analyzing *layer-wise* (L_0, L_1) -smoothness, which combines the benefits of the generalized smoothness model with a structured, anisotropic perspective tailored to the layer-block architecture of neural networks and compatible with arbitrary layer-specific norms. This framework is essential for understanding LMO-based methods like **Muon** and **Scion**.

LMO-based Optimizers. The optimizers **Muon** [16] and **Scion** [29] represent a recent class of methods that have shown strong empirical performance in deep learning. **Muon** was initially introduced as an effective empirical method, with its update rule for hidden layers inspired by ideas from Bernstein and Newhouse [3]. Subsequently, Pethick et al. [29] (authors of **Scion**) explicitly connected these types of updates to the Frank-Wolfe (FW) framework [8, 12], proposing the use of layer-specific norms within an LMO-based update rule. These methods perform updates by solving, for each layer, a linear minimization problem over a norm ball centered at the current iterate. Prior theoretical analyses of these optimizers [20, 22, 29] have relied on standard L -smoothness and analyzed a simplified global update. Our work provides the first convergence guarantees for these methods under the more realistic layer-wise (L_0, L_1) -smoothness, directly addressing their practical layer-wise nature and leveraging the geometric insights offered by LMOs over general norms.

Appendix B. Contributions

We present a comprehensive theoretical and empirical study of a broad class of layer-wise LMO-based optimization algorithms. Our key contributions can be summarized as follows:

- ◊ **A new generalized smoothness framework for deep networks.** We introduce *layer-wise* (L^0, L^1) -smoothness (1), a novel non-Euclidean generalized smoothness condition that reflects the anisotropic, layer-wise structure of modern deep networks. This framework extends standard (L^0, L^1) -smoothness assumption [37] to arbitrary norms while capturing per-layer variation, offering a *realistic foundation for analyzing deep learning optimizers*.
- ◊ **First principled analysis of layer-wise methods.** Building on our new assumption, we develop the first faithful convergence analysis for a class of LMO-based algorithms we term **Gluon** (Algorithms 2 and 1). We recover known algorithms, including state-of-the-art **Muon**-type optimizers, as special cases (3.1 and E.1), and pinpoint why earlier theoretical works *fail* to explain the empirical success of these methods (2). In contrast to prior analyses that oversimplify the update rules used in practice, our framework directly aligns with real-world implementations, bridging a critical gap between theory and application.
- ◊ **Sharper and more general convergence theory.** We develop a convergence theory that extends prior work in both scope and sharpness. In the deterministic case (1), we establish convergence for general non-convex objectives under our 1 (1), and under the block-wise PL condition (9). Unlike earlier analyses, our theory yields *adaptive, layer-wise stepsizes* that align remarkably well with those selected via tuning in large-scale experiments [29] (4). The analysis is extended to the practical stochastic variant in Appendix E, where we prove convergence under a non-Euclidean bounded variance assumption. In both deterministic and stochastic regimes, our guarantees are stronger and more general than all prior work (see 1 in the Appendix for a detailed comparison). While previous theories fail to explain the empirical success of **Muon**-type methods, we are the first to demonstrate their *provable advantage over SGD*, offering *tighter convergence rates* under *more general assumptions* (F). Moreover, we provide the first theoretical explanation of the benefits of layer-wise learning rates, clearly establishing the advantages of structured, anisotropic optimization in deep learning.
- ◊ **Empirical evidence.** We validate our theoretical insights through extensive experiments (4 and G) in both language modeling (NanoGPT on FineWeb) and image classification (CNN on CIFAR-10). The results confirm that our 1 holds approximately throughout training and demonstrate the practical utility of our theoretically prescribed stepsizes from 1.

Appendix C. Auxiliary lemmas

Lemma 2 *Let $f : \mathcal{S} \mapsto \mathbb{R}$ satisfy Assumption 1. Then, for any $X, Y \in \mathcal{S}$, we have*

$$|f(Y) - f(X) - \langle \nabla f(X), Y - X \rangle| \leq \sum_{i=1}^p \frac{L_i^0 + L_i^1 \|\nabla_i f(X)\|_{(i)\star}}{2} \|Y_i - X_i\|_{(i)}^2.$$

Proof For all $X, Y \in \mathcal{S}$ we have

$$\begin{aligned} f(Y) &= f(X) + \int_0^1 \langle \nabla f(X + \tau(Y - X)), Y - X \rangle d\tau \\ &= f(X) + \langle \nabla f(X), Y - X \rangle + \int_0^1 \langle \nabla f(X + \tau(Y - X)) - \nabla f(X), Y - X \rangle d\tau. \end{aligned}$$

Therefore, using the Cauchy-Schwarz inequality and Assumption 1, we obtain

$$\begin{aligned} &|f(Y) - f(X) - \langle \nabla f(X), Y - X \rangle| \\ &\leq \left| \int_0^1 \sum_{i=1}^p \langle \nabla_i f(X + \tau(Y - X)) - \nabla_i f(X), Y_i - X_i \rangle_{(i)} d\tau \right| \\ &\leq \int_0^1 \sum_{i=1}^p \left| \langle \nabla_i f(X + \tau(Y - X)) - \nabla_i f(X), Y_i - X_i \rangle_{(i)} \right| d\tau \\ &\leq \int_0^1 \sum_{i=1}^p \|\nabla_i f(X + \tau(Y - X)) - \nabla_i f(X)\|_{(i)\star} \|Y_i - X_i\|_{(i)} d\tau \\ &\leq \int_0^1 \sum_{i=1}^p \tau (L_i^0 + L_i^1 \|\nabla_i f(X)\|_{(i)\star}) \|Y_i - X_i\|_{(i)}^2 d\tau \\ &= \sum_{i=1}^p \frac{L_i^0 + L_i^1 \|\nabla_i f(X)\|_{(i)\star}}{2} \|Y_i - X_i\|_{(i)}^2. \end{aligned}$$

■

Lemma 3 *Suppose that f is L -smooth with respect to the norm defined in (6), i.e.,*

$$\|\nabla f(X) - \nabla f(Y)\|_{\max\star} \leq L \|X - Y\|_{\max},$$

where $X = [X_1, \dots, X_p]$ and $Y = [Y_1, \dots, Y_p]$ with $X_i, Y_i \in \mathcal{S}_i$. Then 1 holds with $L_i^0 \leq L$ and $L_i^1 = 0$ for all $i = 1, \dots, p$.

Proof L -smoothness and the definition of the norm give

$$\sum_{i=1}^p \|\nabla_i f(X) - \nabla_i f(Y)\|_{(i)\star} \leq L \max \left\{ \|X_1 - Y_1\|_{(1)}, \dots, \|X_p - Y_p\|_{(p)} \right\}$$

for all $X, Y \in \mathcal{S}$. In particular, choosing $X = [X_1, \dots, X_p]$ and $Y = [X_1, \dots, X_{j-1}, Y_j, X_{j+1}, \dots, X_p]$, we have

$$\|\nabla_j f(X) - \nabla_j f(Y)\|_{(j)\star} \leq \sum_{i=1}^p \|\nabla_i f(X) - \nabla_i f(Y)\|_{(i)\star} \leq L \|X_j - Y_j\|_{(j)}$$

for any $j \in \{1, \dots, p\}$, proving the claim. \blacksquare

Lemma 4 Suppose that $x_1, \dots, x_p, y_1, \dots, y_p \in \mathbb{R}$, $\max_{i \in [p]} |x_i| > 0$ and $z_1, \dots, z_p > 0$. Then

$$\sum_{i=1}^p \frac{y_i^2}{z_i} \geq \frac{(\sum_{i=1}^p x_i y_i)^2}{\sum_{i=1}^p z_i x_i^2}.$$

Proof Cauchy-Schwarz inequality gives

$$\left(\sum_{i=1}^p x_i y_i \right)^2 = \left(\sum_{i=1}^p \frac{y_i}{\sqrt{z_i}} \sqrt{z_i} x_i \right)^2 \leq \left(\sum_{i=1}^p \frac{y_i^2}{z_i} \right) \left(\sum_{i=1}^p z_i x_i^2 \right).$$

Rearranging, we obtain the result. \blacksquare

Lemma 5 (Technical Lemma 10 by Hübler et al. [11]) Let $q \in (0, 1)$, $p \geq 0$, and $p \geq q$. Further, let $a, b \in \mathbb{N}_{\geq 2}$ with $a \leq b$. Then

$$\sum_{k=a-1}^{b-1} (1+k)^{-p} \prod_{\tau=a-1}^k (1 - (\tau+1)^{-q}) \leq (a-1)^{q-p} \exp\left(\frac{a^{1-q} - (a-1)^{1-q}}{1-q}\right).$$

Lemma 6 (Technical Lemma 11 by Hübler et al. [11]) Let $t > 0$ and for $k \in \mathbb{N}_{\geq 0}$, set $\beta^k = 1 - (k+1)^{-1/2}$, $t^k = t(k+1)^{-3/4}$, $t > 0$. Then, for all $K \in \mathbb{N}_{\geq 1}$ the following inequalities hold:

$$(i) \sum_{k=0}^{K-1} t^k \sqrt{\sum_{\tau=0}^k (1 - \beta^\tau)^2 \prod_{\kappa=\tau+1}^k (\beta^\kappa)^2} \leq t \left(\frac{7}{2} + \sqrt{2e^2 \log(K)} \right),$$

$$(ii) \sum_{k=0}^{K-1} t^k \sum_{\tau=1}^k t^\tau \prod_{\kappa=\tau}^k \beta^\kappa \leq 7t^2 (3 + \log(K)).$$

Proof This is a direct consequence of Lemma 11 by Hübler et al. [11]. To obtain (ii), it suffices to take the limit as $L^1 \rightarrow 0$ in statement (ii) of part (b). \blacksquare

Appendix D. Remarks on the theoretical results

D.1. Note on radii and stepsizes

It is known (see, e.g., Gruntkowska et al. [10, Theorem D.1], who establish this for $\mathcal{S} = \mathbb{R}^d$ under Euclidean norms; the extension to general normed vector spaces is entirely analogous) that if g is a convex function, then the solution to the problem

$$\arg \min_{X \in \mathcal{B}^k} g(X)$$

is unique and lies on the boundary of the ball $\mathcal{B}^k \stackrel{\text{def}}{=} \{X \in \mathcal{S} : \|X - X^k\| \leq t^k\}$ (unless $\mathcal{B}^k \cap \arg \min_{X \in \mathcal{S}} g(X) \neq \emptyset$).

This applies directly to the LMO subproblem solved at each iteration of **Gluon** in (18), since the objective $\langle M_i^k, X_i \rangle_{(i)}$ is a linear function of X_i , and hence convex. In other words, each LMO step moves the iterate from the center of the ball X_i^k to a new point X_i^{k+1} located on the boundary of \mathcal{B}_i^k , effectively traversing a distance of t_i^k at each step. For this reason, we use the terms *radius*, *stepsize*, and *learning rate* interchangeably.

D.2. Note on prior analyses

As presented, prior convergence results do not directly apply to the algorithms used in practice. However, there is a workaround. Specifically, some of the existing convergence guarantees [20, 29] expressed in terms of the flat vector x are transferable to the structured parameters $X = [X_1, \dots, X_l] \in \mathcal{S}$ by employing the max-norm [2, 21], defined as

$$\|X\|_{\max} \stackrel{\text{def}}{=} \max \left\{ \|X_1\|_{(1)}, \dots, \|X_p\|_{(p)} \right\}, \quad (6)$$

with corresponding dual norm $\|Y\|_{\max \star} = \sup_{\|X\|_{\max} \leq 1} \langle X, Y \rangle = \sum_{i=1}^p \|Y_i\|_{(i)\star}$. Nevertheless, these works do not make this connection explicit, and an additional layer of analysis is required to ensure the guarantees meaningfully extend to the structured practical setting. Even if such a translation was attempted, the global treatment introduces serious practical limitations. For example, real-world training pipelines tune parameters on a per-layer basis, reflecting the heterogeneous structure of deep networks. Max-norm-based guarantees overlook this variability and offer no mechanism for per-layer control in hyperparameter selection.

Table 1: Comparison of convergence guarantees for **Gluon** (Algorithms 2 and 1) to achieve $\min_{k=0,\dots,K-1} \sum_{i=1}^p \mathbb{E}[\|\nabla_i f(X^k)\|_{(i)\star}] \leq \varepsilon$, where the $\mathcal{O}(\cdot)$ notation hides logarithmic factors. Notation: K = total number of iterations, (L^0, L^1) = the result holds under layer-wise (L^0, L^1) -smoothness, t_i^k = radius/stepsizes, $1 - \beta^k$ = momentum.

Result	Stochastic?	(L^0, L^1)	Rate	Stepsizes t_i^k	$1 - \beta^k$
[20, Theorem 1]	✗	✗	$\mathcal{O}\left(\frac{1}{K^{1/2}}\right)$	const $\propto \frac{1}{K^{1/2}}$ ^(b)	—
[20, Theorem 2]	✓	✗	$\mathcal{O}\left(\frac{1}{K^{1/4}}\right)$	const $\propto \frac{1}{K^{3/4}}$ ^(b)	const $\propto \frac{1}{K^{1/2}}$
[22, Theorem 2.1] ^(a)	✓	✗	$\mathcal{O}\left(\frac{1}{K^{1/4}}\right)$	const $\propto \frac{1}{K^{3/4}}$ ^(b)	const $\propto \frac{1}{K^{1/2}}$
[29, Lemma 5.4]	✓	✗	$\mathcal{O}\left(\frac{1}{K^{1/4}}\right)$	$\propto \frac{1}{k^{1/2}}$	
NEW: 1	✗	✓	$\mathcal{O}\left(\frac{1}{K^{1/2}}\right)$	Adaptive	—
NEW: 10	✓	✓	$\mathcal{O}\left(\frac{1}{K^{1/4}}\right)$	$\propto \frac{1}{k^{3/4}}$	$\propto \frac{1}{k^{1/2}}$

^(a) Applies only to the **Muon/Scion** update in (8) with $p = 1$.

^(b) These stepsizes are impractically tiny since they have an inverse dependence on the total number of iterations K .

Algorithm 1: Deterministic Adaptive Layer-Wise LMO-based Optimizer

Data: Initial model parameters $X^0 = [X_1^0, \dots, X_p^0] \in \mathcal{S}$

for $k = 0, 1, \dots, K - 1$ **do**

for $i = 1, 2, \dots, p$ **do**

 Choose adaptive stepsize/radius $t_i^k > 0$ for layer i ;

 Update parameters for layer i via LMO over $\mathcal{B}_i^k \stackrel{\text{def}}{=} \{X_i \in \mathcal{S}_i : \|X_i - X_i^k\|_{(i)} \leq t_i^k\}$;

$$X_i^{k+1} = \text{LMO}_{\mathcal{B}_i^k} \left(\nabla_i f(X^k) \right) \stackrel{\text{def}}{=} \arg \min_{X_i \in \mathcal{B}_i^k} \langle \nabla_i f(X^k), X_i \rangle_{(i)} \quad (7)$$

end

 Update full vector: $X^{k+1} = [X_1^{k+1}, \dots, X_p^{k+1}]$;

end

Appendix E. Deterministic case

We begin by considering the deterministic counterpart of **Gluon**, as formalized in 1. We first review several existing algorithms that fall within this framework (E.1), followed by a proof of 1 (E.2). Finally, we present an additional convergence guarantee under the layer-wise Polyak-Łojasiewicz (PL) condition (E.3).

E.1. Special cases of the LMO framework

As outlined in 3.1, deterministic **Gluon** encompasses a general class of algorithms, parameterized by the choice of norms $\|\cdot\|_{(i)}$ in the LMO. We now provide a more detailed discussion of the most notable special cases.

Layer-wise normalized GD [36]. Let $\|\cdot\|_{(i)} = \|\cdot\|_{2 \rightarrow 2}$ for each parameter group and assume that $n_i = 1$ for all $i = 1, \dots, p$. In this case, the spectral norm reduces to the standard Euclidean norm $\|\cdot\|_2$, yielding the update rule

$$X_i^{k+1} = X_i^k - t_i^k \frac{\nabla_i f(X^k)}{\|\nabla_i f(X^k)\|_2}, \quad i = 1, \dots, p,$$

which corresponds to layer-wise normalized GD. With a suitable choice of t_i^k (see Theorem 1), the method can also recover the Gradient Method for (L^0, L^1) -smooth functions [33].

Layer-wise signGD [1]. Suppose that $\|\cdot\|_{(i)} = \|\cdot\|_{1 \rightarrow \infty}$ for each parameter group, with $n_i = 1$ for all $i = 1, \dots, p$. Then, $\|\cdot\|_{1 \rightarrow \infty}$ reduces to $\|\cdot\|_\infty$, and the update becomes

$$X_i^{k+1} = X_i^k - t_i^k \text{sign}(\nabla_i f(X^k)), \quad i = 1, \dots, p,$$

where the sign function is applied element-wise. This is equivalent to layer-wise signGD.

Muon [16]. Here, the spectral norm $\|\cdot\|_{2 \rightarrow 2}$ is used for all parameter groups, without restrictions on n_i . In this case, it can be shown that (7) is equivalent to

$$X_i^{k+1} = X_i^k - t_i^k U_i^k (V_i^k)^\top, \quad i = 1, \dots, p, \quad (8)$$

where $\nabla_i f(X^k) = U_i^k \Sigma_i^k (V_i^k)^\top$ is the singular value decomposition [3]. This is exactly the per-layer deterministic version of the Muon optimizer. In practical LLM training, a more general variant of (8) incorporating stochasticity and momentum is applied to the intermediate layers, while the input and output layers are optimized using other methods.

Unconstrained Scion [29]. We can also recover two variants of unScion introduced by Pethick et al. [29]: one for training LLMs on next-token prediction, and another for training CNNs for image classification.

- **Training LLMs.** Define the norms $\|\cdot\|_{(i)}$ as follows: for $i = 1, \dots, p-1$, corresponding to weight matrices of transformer blocks, set $\|\cdot\|_{(i)} = \sqrt{n_i/m_i} \|\cdot\|_{2 \rightarrow 2}$, and for the last group X_p , representing the embedding and output layers (which coincide under the weight sharing regime considered here), let $\|\cdot\|_{(p)} = n_p \|\cdot\|_{1 \rightarrow \infty}$. In this case, (7) becomes

$$\begin{aligned} X_i^{k+1} &= X_i^k - t_i^k \sqrt{\frac{m_i}{n_i}} U_i^k (V_i^k)^\top, \quad i = 1, \dots, p-1, \\ X_p^{k+1} &= X_p^k - \frac{t_p^k}{n_p} \text{sign}(\nabla_p f(X^k)), \end{aligned} \quad (9)$$

where $\nabla_i f(X^k) = U_i^k \Sigma_i^k (V_i^k)^\top$ is the singular value decomposition. This is equivalent to deterministic layer-wise unScion optimizer without momentum. A more general variant, incorporating stochasticity and momentum and applied to all layers, was shown by Pethick et al. [29] to outperform Muon on LLM training tasks.

- **Training CNNs.** The main difference in the CNN setting is the presence of not only 2D weight matrices, but also 1D bias vectors and 4D convolutional kernels parameters. Biases are 1D tensors of shape $\mathbb{R}^{C_i^{out}}$, for which we use scaled Euclidean norms. Convolutional parameters (conv) are 4D tensors with shapes $\mathbb{R}^{C_i^{out} \times C_i^{in} \times k \times k}$, where C_i^{out} and C_i^{in} denote the number of output and input channels, and k is the kernel size. To compute norms, we reshape each 4D tensor to a 2D matrix of shape $\mathbb{R}^{C_i^{out} \times C_i^{in} k^2}$, and then apply a scaled $\|\cdot\|_{2 \rightarrow 2}$ norm. This yields the norm choices $\|\cdot\|_{(i)} = \sqrt{1/C_i^{out}} \|\cdot\|_2$ for biases, $\|\cdot\|_{(i)} = k^2 \sqrt{C_i^{in}/C_i^{out}} \|\cdot\|_{2 \rightarrow 2}$ for conv, and $\|\cdot\|_{(p)} = n_p \|\cdot\|_{1 \rightarrow \infty}$ for the last group X_p , associated with classification head weights. Then, it can be shown that (7) is equivalent to

$$\begin{aligned} X_i^{k+1} &= X_i^k - t_i^k \sqrt{C_i^{out}} \frac{\nabla_i f(X^k)}{\|\nabla_i f(X^k)\|_2}, & (\text{for biases}), \\ X_i^{k+1} &= X_i^k - t_i^k \frac{1}{k^2} \sqrt{\frac{C_i^{out}}{C_i^{in}}} U_i^k \left(V_i^k\right)^\top, & (\text{for conv}), \\ X_p^{k+1} &= X_p^k - \frac{t_p^k}{n_p} \text{sign} \left(\nabla_p f(X^k)\right), & (\text{for head}) \end{aligned} \quad (10)$$

where $\nabla_i f(X^k) = U_i^k \Sigma_i^k (V_i^k)^\top$ is the singular value decomposition. This corresponds to the deterministic layer-wise unScion optimizer without momentum.

E.2. Proof of Theorem 1

We now state and prove a generalization of 1.

Theorem 7 *Let 1 hold and fix $\varepsilon > 0$. Let X^0, \dots, X^{K-1} be the iterates of deterministic Gluon (Algorithm 1) run with stepsizes $t_i^k = \frac{\|\nabla_i f(X^k)\|_{(i)\star}}{L_i^0 + L_i^1 \|\nabla_i f(X^k)\|_{(i)\star}}$. Then,*

1. *In order to reach the precision*

$$\min_{k=0, \dots, K-1} \sum_{i=1}^p \left\| \nabla_i f(X^k) \right\|_{(i)\star} \leq \varepsilon,$$

it suffices to run the algorithm for

$$K = \left\lceil \frac{2\Delta^0 \sum_{i=1}^p L_i^0}{\epsilon^2} + \frac{2\Delta^0 L_{\max}^1}{\epsilon} \right\rceil \quad (11)$$

iterations;

2. *In order to reach the precision*

$$\min_{k=0, \dots, K-1} \sum_{i=1}^p \left[\frac{\frac{1}{L_i^1}}{\frac{1}{p} \sum_{j=1}^p \frac{1}{L_j^1}} \left\| \nabla_i f(X^k) \right\|_{(i)\star} \right] \leq \varepsilon, \quad (12)$$

it suffices to run the algorithm for

$$K = \left\lceil \frac{2\Delta^0 \left(\sum_{i=1}^p \frac{L_i^0}{(L_i^1)^2} \right)}{\varepsilon^2 \left(\frac{1}{p} \sum_{j=1}^p \frac{1}{L_j^1} \right)^2} + \frac{2\Delta^0}{\varepsilon \left(\frac{1}{p} \sum_{j=1}^p \frac{1}{L_j^1} \right)} \right\rceil \quad (13)$$

iterations,

where $\Delta^0 \stackrel{\text{def}}{=} f(X^0) - \inf_{X \in \mathcal{S}} f(X)$ and $L_{\max}^1 \stackrel{\text{def}}{=} \max_{i=1,\dots,p} L_i^1$.

Remark 8 Let us compare bounds (11) and (13). Due to the reweighting of the gradient component norms in (12), the rates are not exactly equivalent. Nevertheless, both use weights that sum to p , ensuring a fair comparison. Obviously, $(1/p \sum_{j=1}^p 1/L_j^1)^{-1} \leq L_{\max}^1$ so the second term in (13) is always no worse than its counterpart in (11). The comparison of the first terms, however, depends on how the sequences $\{L_i^0\}$ and $\{L_i^1\}$ relate: if larger values of L_i^0 's tend to be attached to smaller values of L_i^1 , then the first term in (11) improves over that in (13), while for a positive correlation the opposite is true. Indeed, in the extreme case when $L_1^0 \geq \dots \geq L_p^0$ and $L_1^1 \leq \dots \leq L_p^1$ (or the reverse ordering), Chebyshev's sum inequality implies that

$$\frac{\sum_{i=1}^p \frac{L_i^0}{(L_i^1)^2}}{\left(\frac{1}{p} \sum_{j=1}^p \frac{1}{L_j^1} \right)^2} \geq \frac{\left(\frac{1}{p} \sum_{i=1}^p \frac{L_i^0}{L_i^1} \right) \left(\frac{1}{p} \sum_{i=1}^p \frac{1}{L_i^1} \right)}{\frac{1}{p} \left(\frac{1}{p} \sum_{j=1}^p \frac{1}{L_j^1} \right)^2} \geq \frac{\left(\frac{1}{p} \sum_{i=1}^p L_i^0 \right) \left(\frac{1}{p} \sum_{i=1}^p \frac{1}{L_i^1} \right)}{\frac{1}{p} \left(\frac{1}{p} \sum_{j=1}^p \frac{1}{L_j^1} \right)} = \sum_{i=1}^p L_i^0.$$

Conversely, if both sequences $\{L_i^0\}$ and $\{L_i^1\}$ are sorted in the same order (either increasing or decreasing), the inequality reverses, and the first term of (13) may be tighter. That said, empirical evidence we provide in 4 indicates that in practice $L_i^0 \approx 0$ across all layers, in which case the first terms in (11) and (13) effectively vanish. Then, (13) is clearly superior, replacing the worst-case constant L_{\max}^1 by the harmonic mean.

Proof We start with the result obtained in Lemma 2 with $X = X^k$ and $Y = X^{k+1}$

$$\begin{aligned} f(X^{k+1}) &\leq f(X^k) + \left\langle \nabla f(X^k), X^{k+1} - X^k \right\rangle + \sum_{i=1}^p \frac{L_i^0 + L_i^1 \|\nabla_i f(X^k)\|_{(i)\star}}{2} \|X_i^k - X_i^{k+1}\|_{(i)}^2 \\ &= f(X^k) + \sum_{i=1}^p \left[\left\langle \nabla_i f(X^k), X_i^{k+1} - X_i^k \right\rangle_{(i)} + \frac{L_i^0 + L_i^1 \|\nabla_i f(X^k)\|_{(i)\star}}{2} \|X_i^k - X_i^{k+1}\|_{(i)}^2 \right]. \end{aligned}$$

The update rule (7) and the definition of the dual norm $\|\cdot\|_{(i)\star}$ give

$$\|X_i^k - X_i^{k+1}\|_{(i)}^2 \leq (t_i^k)^2$$

and

$$\begin{aligned} \left\langle \nabla_i f(X^k), X_i^{k+1} - X_i^k \right\rangle_{(i)} &= \left\langle \nabla_i f(X^k), \text{LMO}_{\mathcal{B}_i^k}(\nabla_i f(X^k)) - X_i^k \right\rangle_{(i)} \\ &= -t_i^k \max_{\|X_i\|_{(i)} \leq 1} \left\langle \nabla_i f(X^k), X_i \right\rangle_{(i)} \\ &= -t_i^k \|\nabla_i f(X^k)\|_{(i)\star}. \end{aligned}$$

Consequently,

$$f(X^{k+1}) \leq f(X^k) + \sum_{i=1}^p \left[-t_i^k \|\nabla_i f(X^k)\|_{(i)\star} + \frac{L_i^0 + L_i^1 \|\nabla_i f(X^k)\|_{(i)\star}}{2} (t_i^k)^2 \right].$$

Now, choosing

$$t_i^k = \frac{\|\nabla_i f(X^k)\|_{(i)\star}}{L_i^0 + L_i^1 \|\nabla_i f(X^k)\|_{(i)\star}},$$

which minimizes the right-hand side of the last inequality, yields the descent inequality

$$f(X^{k+1}) \leq f(X^k) - \sum_{i=1}^p \frac{\|\nabla_i f(X^k)\|_{(i)\star}^2}{2(L_i^0 + L_i^1 \|\nabla_i f(X^k)\|_{(i)\star})}. \quad (14)$$

Summing the terms, we obtain

$$\begin{aligned} \sum_{k=0}^{K-1} \sum_{i=1}^p \frac{\|\nabla_i f(X^k)\|_{(i)\star}^2}{2(L_i^0 + L_i^1 \|\nabla_i f(X^k)\|_{(i)\star})} &\leq \sum_{k=0}^{K-1} (f(X^k) - f(X^{k+1})) \\ &= f(X^0) - f(X^K) \\ &\leq f(X^0) - \inf_{X \in \mathcal{S}} f(X) =: \Delta^0. \end{aligned} \quad (15)$$

Now, the analysis can proceed in two ways:

1. Upper-bounding L_i^1 by $L_{\max}^1 := \max_{i=1,\dots,p} L_i^1$ in (15), we obtain

$$\sum_{k=0}^{K-1} \sum_{i=1}^p \frac{\|\nabla_i f(X^k)\|_{(i)\star}^2}{2(L_i^0 + L_{\max}^1 \|\nabla_i f(X^k)\|_{(i)\star})} \leq \Delta^0. \quad (16)$$

Now, applying 4 with $x_i = 1$, $y_i = \|\nabla_i f(X^k)\|_{(i)\star}$ and $z_i = 2(L_i^0 + L_{\max}^1 \|\nabla_i f(X^k)\|_{(i)\star})$ gives

$$\begin{aligned} \phi \left(\sum_{i=1}^p \|\nabla_i f(X^k)\|_{(i)\star} \right) &= \frac{(\sum_{i=1}^p \|\nabla_i f(X^k)\|_{(i)\star})^2}{2(\sum_{i=1}^p L_i^0 + L_{\max}^1 \sum_{i=1}^p \|\nabla_i f(X^k)\|_{(i)\star})} \\ &\leq \sum_{i=1}^p \frac{\|\nabla_i f(X^k)\|_{(i)\star}^2}{2(L_i^0 + L_{\max}^1 \|\nabla_i f(X^k)\|_{(i)\star})}, \end{aligned}$$

where $\phi(t) \stackrel{\text{def}}{=} \frac{t^2}{2(\sum_{i=1}^p L_i^0 + L_{\max}^1 t)}$. Combining the last inequality with (16) and using the fact that ϕ is increasing, we obtain

$$K \phi \left(\min_{k=0,\dots,K-1} \sum_{i=1}^p \|\nabla_i f(X^k)\|_{(i)\star} \right) \leq \sum_{k=0}^{K-1} \phi \left(\sum_{i=1}^p \|\nabla_i f(X^k)\|_{(i)\star} \right) \leq \Delta^0, \quad (17)$$

and hence

$$\min_{k=0,\dots,K-1} \sum_{i=1}^p \|\nabla_i f(X^k)\|_{(i)\star} \leq \phi^{-1} \left(\frac{\Delta^0}{K} \right),$$

where ϕ^{-1} is the inverse function (which exists since ϕ is increasing). Therefore, to reach the precision $\min_{k=0,\dots,K-1} \sum_{i=1}^p \|\nabla_i f(X^k)\|_{(i)\star} \leq \epsilon$, it is sufficient to choose the number of iterations to be

$$K = \left\lceil \frac{\Delta^0}{\phi(\epsilon)} \right\rceil = \left\lceil \frac{2 \sum_{i=1}^p L_i^0 \Delta^0}{\epsilon^2} + \frac{2L_{\max}^1 \Delta^0}{\epsilon} \right\rceil.$$

2. Alternatively, we can start from the inequality (15) and apply 4 with $x_i = 1/L_i^1$, $y_i = \|\nabla_i f(X^k)\|_{(i)\star}$ and $z_i = 2(L_i^0 + L_i^1 \|\nabla_i f(X^k)\|_{(i)\star})$ to obtain

$$\begin{aligned} \Delta^0 &\geq \sum_{k=0}^{K-1} \sum_{i=1}^p \frac{\|\nabla_i f(X^k)\|_{(i)\star}^2}{2(L_i^0 + L_i^1 \|\nabla_i f(X^k)\|_{(i)\star})} \\ &\geq \sum_{k=0}^{K-1} \frac{\left(\sum_{i=1}^p \frac{1}{L_i^1} \|\nabla_i f(X^k)\|_{(i)\star} \right)^2}{2 \left(\sum_{i=1}^p \frac{1}{(L_i^1)^2} (L_i^0 + L_i^1 \|\nabla_i f(X^k)\|_{(i)\star}) \right)} \\ &= \sum_{k=0}^{K-1} \frac{\left(\sum_{i=1}^p \frac{1}{L_i^1} \|\nabla_i f(X^k)\|_{(i)\star} \right)^2}{2 \left(\sum_{i=1}^p \frac{L_i^0}{(L_i^1)^2} + \sum_{i=1}^p \frac{1}{L_i^1} \|\nabla_i f(X^k)\|_{(i)\star} \right)} \\ &= \sum_{t=0}^{K-1} \psi \left(\sum_{i=1}^p \frac{1}{L_i^1} \|\nabla_i f(X^k)\|_{(i)\star} \right), \end{aligned}$$

where $\psi(t) \stackrel{\text{def}}{=} \frac{t^2}{2 \left(\sum_{i=1}^p \frac{L_i^0}{(L_i^1)^2} + t \right)}$. Since the function ψ is increasing for $t > 0$, ψ^{-1} exists. It follows that

$$\begin{aligned} \Delta^0 &\geq \sum_{k=0}^{K-1} \psi \left(\sum_{i=1}^p \frac{1}{L_i^1} \|\nabla_i f(X^k)\|_{(i)\star} \right) \\ &\geq K \psi \left(\min_{k=0,\dots,K-1} \sum_{i=1}^p \frac{1}{L_i^1} \|\nabla_i f(X^k)\|_{(i)\star} \right), \end{aligned}$$

and hence

$$\min_{k=0,\dots,K-1} \sum_{i=1}^p \frac{1}{L_i^1} \|\nabla_i f(X^k)\|_{(i)\star} \leq \psi^{-1} \left(\frac{\Delta^0}{K} \right).$$

This in turn means that to reach the precision

$$\min_{k=0,\dots,K-1} \sum_{i=1}^p \left[\frac{\frac{1}{L_i^1}}{\frac{1}{p} \sum_{j=1}^p \frac{1}{L_j^1}} \|\nabla_i f(X^k)\|_{(i)\star} \right] \leq \varepsilon,$$

it suffices to run the algorithm for

$$K = \left\lceil \frac{\Delta^0}{\psi \left(\varepsilon \left(\frac{1}{p} \sum_{j=1}^p \frac{1}{L_j^1} \right) \right)} \right\rceil = \left\lceil \frac{2\Delta^0 \left(\sum_{i=1}^p \frac{L_i^0}{(L_i^1)^2} \right)}{\varepsilon^2 \left(\frac{1}{p} \sum_{j=1}^p \frac{1}{L_j^1} \right)^2} + \frac{2\Delta^0}{\varepsilon \left(\frac{1}{p} \sum_{j=1}^p \frac{1}{L_j^1} \right)} \right\rceil$$

iterations. ■

E.3. Convergence under the PŁ condition

We now establish convergence rates under the layer-wise Polyak–Łojasiewicz (PŁ) condition, introduced in Assumption 2. This property is especially relevant for heavily over-parameterized neural networks, as it has been shown to capture the properties of their loss landscapes [23].

Assumption 2 (Layer-wise Polyak–Łojasiewicz condition) *The function $f : \mathcal{S} \mapsto \mathbb{R}$ satisfies the layer-wise Polyak–Łojasiewicz (PŁ) condition with a constant $\mu > 0$, i.e., for any $X \in \mathcal{S}$*

$$\sum_{i=1}^p \|\nabla_i f(X)\|_{(i)*}^2 \geq 2\mu (f(X) - f^*),$$

where $f^* := \inf_{X \in \mathcal{S}} f(X) > -\infty$.

Assumption 2 reduces to the standard PŁ condition [17] by vectorizing the parameters and adopting the Euclidean norm $\|\cdot\|_2$.

Theorem 9 *Let Assumptions 1 and 2 hold and fix $\varepsilon > 0$. Let X^0, \dots, X^{K-1} be the iterates of deterministic Gluon (Algorithm 1) run with $t_i^k = \frac{\|\nabla_i f(X^k)\|_{(i)*}}{L_i^0 + L_i^1 \|\nabla_i f(X^k)\|_{(i)*}}$.*

1. *If $L_i^1 \geq 0$, then to reach the precision $\min_{k=0, \dots, K-1} f(X^k) - f^* \leq \epsilon$, it suffices to run the algorithm for*

$$K = \left\lceil \frac{\sum_{i=1}^p L_i^0 \Delta^0}{\mu \epsilon} + \frac{\sqrt{2} L_{\max}^1 \Delta^0}{\sqrt{\mu \epsilon}} \right\rceil$$

iterations,

2. *If $L_i^1 = 0$ for all $i = 1, \dots, p$, then to reach the precision $f(X^K) - f^* \leq \epsilon$, it suffices to run the algorithm for*

$$K = \left\lceil \frac{L_{\max}^0}{\mu} \log \frac{\Delta^0}{\epsilon} \right\rceil,$$

where $L_{\max}^0 := \max_{i=1, \dots, p} L_i^0$, $L_{\max}^1 := \max_{i=1, \dots, p} L_i^1$, $\Delta^0 := f(X^0) - f^*$ and $f^* := \inf_{X \in \mathcal{S}} f(X)$.

Proof We consider two scenarios: (1) the general case with arbitrary $L_i^1 \geq 0$ and (2) $L_i^1 = 0$ for all $i = 1, \dots, p$.

Case 1: $L_i^1 \geq 0$. We start by following the same steps as in the proof of Theorem 1. From (17), we have

$$\sum_{k=0}^{K-1} \phi \left(\sum_{i=1}^p \|\nabla_i f(X^k)\|_{(i)\star} \right) \leq \Delta^0,$$

where $\phi(t) := \frac{t^2}{2(\sum_{i=1}^p L_i^0 + L_{\max}^1 t)}$. Now, using Assumption 2, we get

$$\left(\sum_{i=1}^p \|\nabla_i f(X^k)\|_{(i)\star} \right)^2 \geq \sum_{i=1}^p \|\nabla_i f(X^k)\|_{(i)\star}^2 \geq 2\mu (f(X^k) - f^*).$$

Consequently, since ϕ is an increasing function,

$$\begin{aligned} K\phi \left(\sqrt{2\mu} \sqrt{f(X^{k^*}) - f^*} \right) &\leq \sum_{k=0}^{K-1} \phi \left(\sqrt{2\mu} \sqrt{f(X^k) - f^*} \right) \\ &\leq \sum_{k=0}^{K-1} \phi \left(\sum_{i=1}^p \|\nabla_i f(X^k)\|_{(i)\star} \right) \leq \Delta^0, \end{aligned}$$

where $k^* := \operatorname{argmin}_{k=0, \dots, K-1} f(X^k) - f^*$. Denoting the corresponding inverse function (which exists since ϕ is increasing) by ϕ^{-1} , it follows that

$$\sqrt{2\mu} \sqrt{f(X^{k^*}) - f^*} \leq \phi^{-1} \left(\frac{\Delta^0}{K} \right) \leq \sqrt{2\mu\epsilon}.$$

Therefore, to reach the precision $f(X^{k^*}) - f^* \leq \epsilon$, it is sufficient to choose the number of iterations

$$K = \left\lceil \frac{\Delta^0}{\phi(\sqrt{2\mu\epsilon})} \right\rceil = \left\lceil \frac{\sum_{i=1}^p L_i^0 \Delta^0}{\mu\epsilon} + \frac{\sqrt{2}L_{\max}^1 \Delta^0}{\sqrt{\mu\epsilon}} \right\rceil.$$

Case 2: $L_i^1 = 0$. Inequality (14) from the proof of Theorem 1 with $L_i^1 = 0$ gives

$$f(X^{k+1}) \leq f(X^k) - \sum_{i=1}^p \frac{\|\nabla_i f(X^k)\|_{(i)\star}^2}{2L_i^0}.$$

Using the fact that

$$\sum_{i=1}^p \frac{\|\nabla_i f(X^k)\|_{(i)\star}^2}{2L_i^0} \geq \min_{j=1, \dots, p} \frac{1}{2L_j^0} \sum_{i=1}^p \|\nabla_i f(X^k)\|_{(i)\star}^2 = \frac{1}{2 \max_{j=1, \dots, p} L_j^0} \sum_{i=1}^p \|\nabla f(X^k)\|_{(i)\star}^2$$

along with Assumption 2, we obtain

$$f(X^{k+1}) \leq f(X^k) - \frac{\mu}{L_{\max}^0} (f(X^k) - f^*).$$

The remaining part of the proof follows from the simple observation

$$\log\left(\frac{\Delta_0}{\epsilon}\right) \leq k \frac{\mu}{L_{\max}^0} \leq k \log\left(\frac{1}{1 - \frac{\mu}{L_{\max}^0}}\right).$$

■

Algorithm 2: *Gluon*: Stochastic Adaptive Layer-Wise LMO-based Optimizer with Momentum

Data: Initial model parameters $X^0 = [X_1^0, \dots, X_p^0] \in \mathcal{S}$, momentum $M^0 = [M_1^0, \dots, M_p^0] \in \mathcal{S}$, momentum decay factors $\beta^k \in [0, 1)$ for all iterations $k \geq 0$

for $k = 0, 1, 2, \dots, K-1$ **do**

- Sample $\xi^k \sim \mathcal{D}$;
- for** $i = 1, 2, \dots, p$ **do**

 - Compute stochastic gradient $\nabla_i f_{\xi^k}(X^k)$ for layer i ;
 - Update momentum $M_i^k = \beta^k M_i^{k-1} + (1 - \beta^k) \nabla_i f_{\xi^k}(X^k)$ for layer i ;
 - Choose adaptive stepsize/radius $t_i^k > 0$ for layer i ;
 - Update parameters for layer i via LMO over $\mathcal{B}_i^k \stackrel{\text{def}}{=} \{X_i \in \mathcal{S}_i : \|X_i - X_i^k\|_{(i)} \leq t_i^k\}$;
 - $$X_i^{k+1} = \text{LMO}_{\mathcal{B}_i^k}(M_i^k) := \arg \min_{X_i \in \mathcal{B}_i^k} \langle M_i^k, X_i \rangle_{(i)} \quad (18)$$

- end**
- Update full parameter vector $X^{k+1} = [X_1^{k+1}, \dots, X_p^{k+1}]$;

end

Appendix F. Stochastic case

In practice, computing full gradients is often infeasible due to the scale of modern ML problems. We therefore turn to the practical *Gluon* (2), a stochastic variant of 1 that operates with noisy gradient estimates available through a stochastic gradient oracle $\nabla f_{\xi}, \xi \sim \mathcal{D}$.

Assumption 3 *The stochastic gradient estimator $\nabla f_{\xi} : \mathcal{S} \mapsto \mathcal{S}$ is unbiased and has bounded variance. That is, $\mathbb{E}_{\xi \sim \mathcal{D}}[\nabla f_{\xi}(X)] = \nabla f(X)$ for all $X \in \mathcal{S}$ and there exists $\sigma \geq 0$ such that*

$$\mathbb{E}_{\xi \sim \mathcal{D}}[\|\nabla_i f_{\xi}(X) - \nabla_i f(X)\|_{(i)\star}^2] \leq \sigma^2, \quad \forall X \in \mathcal{S}, i = 1, \dots, p.$$

Note that the choice of norm in 3 is not restrictive: in finite-dimensional spaces, all norms are equivalent, so variance bounds remain valid up to a constant factor when compared to those based on the standard Euclidean norm. The following result establishes the convergence properties.

Theorem 10 *Let Assumptions 1 and 3 hold and fix $\varepsilon > 0$. Let X^0, \dots, X^{K-1} be the iterates of *Gluon* (Algorithm 2) run with $\beta^k = 1 - (k+1)^{-1/2}$, $t_i^k = t_i(k+1)^{-3/4}$ for some $t_i > 0$, and $M_i^0 = \nabla_i f_{\xi^0}(X^0)$. Then*

$$\min_{k=0, \dots, K-1} \sum_{i=1}^p \frac{1}{12L_i^1} \mathbb{E}[\|\nabla_i f(X^k)\|_{(i)\star}] \lesssim \frac{\Delta^0}{K^{1/4}} + \frac{1}{K^{1/4}} \sum_{i=1}^p \left[\frac{\sigma}{L_i^1} + \frac{L_i^0}{(L_i^1)^2} \right], \quad (19)$$

where $\Delta^0 := f(X^0) - f^{\inf}$ and the notation \lesssim hides numerical constants and logarithmic factors.

For $p = 1$, our rate in (19) recovers the complexity for finding a stationary point of (L^0, L^1) -smooth functions established by Hübler et al. [11] for normalized SGD with momentum. When $p \geq 1$, compared to existing guarantees for *Gluon*, our 10 operates under the significantly more general 1

and uniquely supports training with larger, non-constant stepsizes $t_i^k \propto k^{-3/4}$. In contrast, prior analyses prescribe constant, vanishingly small stepsizes $t_i^k \equiv t_i \propto K^{-3/4}$, tied to the *total* number of iterations K (see 1).

F.1. Adaptive stepsizes

Before proving the main result from F, we first present an attempt to formulate an adaptive stepsize strategy for the stochastic setting. This requires the following assumption:

Assumption 4 *The stochastic gradient estimator $\nabla f_\xi : \mathcal{S} \mapsto \mathcal{S}$ is unbiased and has bounded relative variance. That is, $\mathbb{E}[\nabla f_\xi(X)] = \nabla f(X)$ for all $X \in \mathcal{S}$ and there exists $0 \leq \zeta < 1$ such that*

$$\|\nabla_i f_\xi(X) - \nabla_i f(X)\|_{(i)\star} \leq \zeta \|\nabla_i f_\xi(X)\|_{(i)\star}, \quad i = 1, \dots, p$$

holds almost surely for all $X \in \mathcal{S}$.

This assumption is somewhat unconventional due to the presence of the stochastic gradients on the right-hand side of the inequality. It does not follow from standard conditions and does not fall within known frameworks for modeling stochasticity, such as the ABC inequality of Khaled and Richtárik [18]. Instead, it introduces a novel structure with parallels to the literature on contractive compression [5, 7].

To elaborate, recall the definition of a contractive compressor:

Definition 11 (Contractive compressor) *A stochastic mapping $\mathcal{C} : \mathcal{S} \rightarrow \mathcal{S}$ is called a contractive compressor if there exists $\alpha \in [0, 1)$ such that*

$$\mathbb{E} [\|\mathcal{C}(X) - X\|^2] \leq (1 - \alpha) \|X\|^2 \tag{20}$$

for any $X \in \mathcal{S}$.

There is a conceptual similarity between 4 and the contractive property in (20). 4 can be interpreted as asserting that the true gradient $\nabla f(X)$ is effectively a contraction of the stochastic gradient $\nabla f_\xi(X)$, with contraction factor $1 - \zeta$. Unlike contractive compressors, there is no explicit mapping from $\nabla f_\xi(X)$ to $\nabla f(X)$, and the uniform bound implies the same contraction-like behavior across all stochastic gradients.

Although 4 is admittedly strong, it allows us to establish a convergence theorem using an adaptive stepsize strategy similar to the one employed in the deterministic case in 7.

Theorem 12 *Let Assumptions 1 and 4 hold and fix $\varepsilon > 0$. Let X^0, \dots, X^{K-1} be the iterates of Gluon (Algorithm 2) run with $\beta^k = 0$ and $t_i^k = \frac{(1-\zeta)\|\nabla_i f_\xi^k(X^k)\|_{(i)\star}}{L_i^0 + (1+\zeta)L_i^1\|\nabla_i f_\xi^k(X^k)\|_{(i)\star}}$. Then,*

1. *In order to reach the precision*

$$\min_{k=0, \dots, K-1} \sum_{i=1}^p \mathbb{E} \left[\left\| \nabla_i f(X^k) \right\|_{(i)\star} \right] \leq \epsilon,$$

it suffices to run the algorithm for

$$K = \left\lceil \frac{2 \sum_{i=1}^p L_i^0 \Delta^0}{(1 - \zeta)^2 \epsilon^2} + \frac{2(1 + \zeta)L_{\max}^1 \Delta^0}{(1 - \zeta)^2 \epsilon} \right\rceil$$

iterations.

2. In order to reach the precision

$$\min_{k=0, \dots, K-1} \sum_{i=1}^p \left[\frac{\frac{1}{L_i^1}}{\frac{1}{p} \sum_{j=1}^p \frac{1}{L_j^1}} \|\nabla_i f(X^k)\|_{(i)\star} \right] \leq \varepsilon,$$

it suffices to run the algorithm for

$$K = \left\lceil \frac{2\Delta^0 \sum_{i=1}^p \frac{L_i^0}{(L_i^1)^2}}{\varepsilon^2 (1-\zeta)^2 \left(\frac{1}{p} \sum_{j=1}^p \frac{1}{L_j^1} \right)^2} + \frac{2\Delta^0 (1+\zeta)}{\varepsilon (1-\zeta)^2 \left(\frac{1}{p} \sum_{j=1}^p \frac{1}{L_j^1} \right)} \right\rceil$$

iterations,

where $\Delta^0 \stackrel{\text{def}}{=} f(X^0) - \inf_{X \in \mathcal{S}} f(X)$ and $L_{\max}^1 \stackrel{\text{def}}{=} \max_{i=1, \dots, p} L_i^1$.

Proof Lemma 2 with $X = X^k$ and $Y = X^{k+1}$ gives

$$\begin{aligned} & f(X^{k+1}) \\ & \leq f(X^k) + \left\langle \nabla f(X^k), X^{k+1} - X^k \right\rangle + \sum_{i=1}^p \frac{L_i^0 + L_i^1 \|\nabla_i f(X^k)\|_{(i)\star}}{2} \|X_i^k - X_i^{k+1}\|_{(i)}^2 \\ & = f(X^k) + \sum_{i=1}^p \left[\left\langle \nabla_i f(X^k), X_i^{k+1} - X_i^k \right\rangle_{(i)} + \frac{L_i^0 + L_i^1 \|\nabla_i f(X^k)\|_{(i)\star}}{2} \|X_i^k - X_i^{k+1}\|_{(i)}^2 \right] \\ & = f(X^k) + \sum_{i=1}^p \left[\left\langle \nabla_i f_{\xi^k}(X^k), X_i^{k+1} - X_i^k \right\rangle_{(i)} + \left\langle \nabla_i f(X^k) - \nabla_i f_{\xi^k}(X^k), X_i^{k+1} - X_i^k \right\rangle_{(i)} \right] \\ & \quad + \sum_{i=1}^p \frac{L_i^0 + L_i^1 \|\nabla_i f(X^k)\|_{(i)\star}}{2} \|X_i^k - X_i^{k+1}\|_{(i)}^2, \end{aligned}$$

and applying the Cauchy-Schwarz inequality, we get

$$\begin{aligned} f(X^{k+1}) & \leq f(X^k) + \sum_{i=1}^p \left[\left\langle \nabla_i f_{\xi^k}(X^k), X_i^{k+1} - X_i^k \right\rangle_{(i)} \right. \\ & \quad + \|\nabla_i f(X^k) - \nabla_i f_{\xi^k}(X^k)\|_{(i)\star} \|X_i^{k+1} - X_i^k\|_{(i)} \\ & \quad \left. + \frac{L_i^0 + L_i^1 \|\nabla_i f(X^k)\|_{(i)\star}}{2} \|X_i^k - X_i^{k+1}\|_{(i)}^2 \right]. \end{aligned}$$

The update rule (18) and the definition of the dual norm $\|\cdot\|_{(i)\star}$ give

$$\|X_i^k - X_i^{k+1}\|_{(i)}^2 \leq (t_i^k)^2$$

and

$$\begin{aligned}
 \left\langle \nabla_i f_{\xi^k}(X^k), X_i^{k+1} - X_i^k \right\rangle_{(i)} &= \left\langle \nabla_i f_{\xi^k}(X^k), \text{LMO}_{\mathcal{B}_i^k} \left(\nabla_i f_{\xi^k}(X^k) \right) - X_i^k \right\rangle_{(i)} \\
 &= -t_i^k \max_{\|X_i\|_{(i)} \leq 1} \left\langle \nabla_i f_{\xi^k}(X^k), X_i \right\rangle_{(i)} \\
 &= -t_i^k \|\nabla_i f_{\xi^k}(X^k)\|_{(i)\star}.
 \end{aligned}$$

Consequently, using Assumption 4, we obtain

$$\begin{aligned}
 f(X^{k+1}) &\leq f(X^k) + \sum_{i=1}^p \left[-t_i^k \|\nabla_i f_{\xi^k}(X^k)\|_{(i)\star} + t_i^k \|\nabla_i f(X^k) - \nabla_i f_{\xi^k}(X^k)\|_{(i)\star} \right. \\
 &\quad \left. + \frac{L_i^0 + L_i^1 \|\nabla_i f(X^k)\|_{(i)\star}}{2} (t_i^k)^2 \right] \\
 &\leq f(X^k) + \sum_{i=1}^p \left[-(1 - \zeta) t_i^k \|\nabla_i f_{\xi^k}(X^k)\|_{(i)\star} \right. \\
 &\quad \left. + \frac{L_i^0 + (1 + \zeta)L_i^1 \|\nabla_i f_{\xi^k}(X^k)\|_{(i)\star}}{2} (t_i^k)^2 \right].
 \end{aligned}$$

Minimizing the right-hand side of the last inequality with respect to t_i^k yields

$$t_i^k = \frac{(1 - \zeta) \|\nabla_i f_{\xi^k}(X^k)\|_{(i)\star}}{L_i^0 + (1 + \zeta)L_i^1 \|\nabla_i f_{\xi^k}(X^k)\|_{(i)\star}}.$$

This greedy approach for choosing t_i^k gives the descent inequality

$$f(X^{k+1}) \leq f(X^k) - \sum_{i=1}^p \frac{(1 - \zeta)^2 \|\nabla_i f_{\xi^k}(X^k)\|_{(i)\star}^2}{2(L_i^0 + (1 + \zeta)L_i^1 \|\nabla_i f_{\xi^k}(X^k)\|_{(i)\star})}.$$

Taking expectations, we have

$$\mathbb{E}[f(X^{k+1})] \leq \mathbb{E}[f(X^k)] - \sum_{i=1}^p \mathbb{E} \left[\frac{(1 - \zeta)^2 \|\nabla_i f_{\xi^k}(X^k)\|_{(i)\star}^2}{2(L_i^0 + (1 + \zeta)L_i^1 \|\nabla_i f_{\xi^k}(X^k)\|_{(i)\star})} \right]. \quad (21)$$

Now, let us define the function $\phi_i(t) := \frac{(1 - \zeta)^2 t^2}{2(L_i^0 + (1 + \zeta)L_i^1 t)}$. Since $\phi_i(t)$ is convex, Jensen's inequality gives

$$\begin{aligned}
 \mathbb{E}[f(X^k)] - \mathbb{E}[f(X^{k+1})] &\geq \sum_{i=1}^p \mathbb{E} \left[\frac{(1 - \zeta)^2 \|\nabla_i f_{\xi^k}(X^k)\|_{(i)\star}^2}{2(L_i^0 + (1 + \zeta)L_i^1 \|\nabla_i f_{\xi^k}(X^k)\|_{(i)\star})} \right] \\
 &\geq \sum_{i=1}^p \frac{(1 - \zeta)^2 (\mathbb{E} [\|\nabla_i f_{\xi^k}(X^k)\|_{(i)\star}])^2}{2(L_i^0 + (1 + \zeta)L_i^1 \mathbb{E} [\|\nabla_i f_{\xi^k}(X^k)\|_{(i)\star}])}.
 \end{aligned}$$

By Jensen's inequality and 4

$$\begin{aligned}\mathbb{E} \left[\left\| \nabla_i f(X^k) \right\|_{(i)\star} \right] &= \mathbb{E} \left[\left\| \mathbb{E} \left[\nabla_i f_{\xi_k}(X^k) \mid X^k \right] \right\|_{(i)\star} \right] \\ &\leq \mathbb{E} \left[\mathbb{E} \left[\left\| \nabla_i f_{\xi_k}(X^k) \right\|_{(i)\star} \mid X^k \right] \right] \\ &= \mathbb{E} \left[\left\| \nabla_i f_{\xi_k}(X^k) \right\|_{(i)\star} \right],\end{aligned}$$

and hence, using the fact that ϕ_i is increasing, we get

$$\mathbb{E}[f(X^k)] - \mathbb{E}[f(X^{k+1})] \geq \sum_{i=1}^p \frac{(1-\zeta)^2 \left(\mathbb{E} \left[\left\| \nabla_i f(X^k) \right\|_{(i)\star} \right] \right)^2}{2 \left(L_i^0 + (1+\zeta) L_i^1 \mathbb{E} \left[\left\| \nabla_i f(X^k) \right\|_{(i)\star} \right] \right)}.$$

Summing the terms gives

$$\begin{aligned}\sum_{k=0}^{K-1} \sum_{i=1}^p \frac{(1-\zeta)^2 \left(\mathbb{E} \left[\left\| \nabla_i f(X^k) \right\|_{(i)\star} \right] \right)^2}{2 \left(L_i^0 + (1+\zeta) L_i^1 \mathbb{E} \left[\left\| \nabla_i f(X^k) \right\|_{(i)\star} \right] \right)} &\leq \sum_{k=0}^{K-1} \left(\mathbb{E}[f(X^k)] - \mathbb{E}[f(X^{k+1})] \right) \\ &= \mathbb{E}[f(X^0)] - \mathbb{E}[f(X^K)] \\ &\leq f(X^0) - \inf_{X \in \mathcal{S}} f(X) =: \Delta^0,\end{aligned}\tag{22}$$

The remaining part of the proof closely follows the proof of Theorem 7. We can proceed in two ways:

1. Upper-bounding L_i^1 by $L_{\max}^1 := \max_{i=1,\dots,p} L_i^1$ in (22), we obtain

$$\sum_{k=0}^{K-1} \sum_{i=1}^p \frac{(1-\zeta)^2 \left(\mathbb{E} \left[\left\| \nabla_i f(X^k) \right\|_{(i)\star} \right] \right)^2}{2 \left(L_i^0 + (1+\zeta) L_{\max}^1 \mathbb{E} \left[\left\| \nabla_i f(X^k) \right\|_{(i)\star} \right] \right)} \leq \Delta^0.\tag{23}$$

Now, 4 with $x_i = 1$, $y_i = (1-\zeta) \mathbb{E} \left[\left\| \nabla_i f(X^k) \right\|_{(i)\star} \right]$ and $z_i = 2 \left(L_i^0 + (1+\zeta) L_{\max}^1 \mathbb{E} \left[\left\| \nabla_i f(X^k) \right\|_{(i)\star} \right] \right)$ gives

$$\begin{aligned}\phi \left(\sum_{i=1}^p \mathbb{E} \left[\left\| \nabla_i f(X^k) \right\|_{(i)\star} \right] \right) &= \frac{\left((1-\zeta) \sum_{i=1}^p \mathbb{E} \left[\left\| \nabla_i f(X^k) \right\|_{(i)\star} \right] \right)^2}{2 \sum_{i=1}^p \left(L_i^0 + (1+\zeta) L_{\max}^1 \mathbb{E} \left[\left\| \nabla_i f(X^k) \right\|_{(i)\star} \right] \right)} \\ &\leq \sum_{i=1}^p \frac{(1-\zeta)^2 \mathbb{E} \left[\left\| \nabla_i f(X^k) \right\|_{(i)\star} \right]^2}{2 \left(L_i^0 + (1+\zeta) L_{\max}^1 \mathbb{E} \left[\left\| \nabla_i f(X^k) \right\|_{(i)\star} \right] \right)}\end{aligned}$$

where $\phi(t) \stackrel{\text{def}}{=} \frac{(1-\zeta)^2 t^2}{2(\sum_{i=1}^p L_i^0 + (1+\zeta) L_{\max}^1 t)}$. Combining the last inequality with (23) and using the fact that ϕ is increasing, we get

$$K \phi \left(\min_{k=0,\dots,K-1} \sum_{i=1}^p \mathbb{E} \left[\left\| \nabla_i f(X^k) \right\|_{(i)\star} \right] \right) \leq \sum_{k=0}^{K-1} \phi \left(\sum_{i=1}^p \mathbb{E} \left[\left\| \nabla_i f(X^k) \right\|_{(i)\star} \right] \right) \leq \Delta^0.$$

and hence

$$\min_{k=0, \dots, K-1} \sum_{i=1}^p \mathbb{E} \left[\|\nabla_i f(X^k)\|_{(i)\star} \right] \leq \phi^{-1} \left(\frac{\Delta^0}{K} \right),$$

where ϕ^{-1} denotes the inverse function (which exists since ϕ is increasing). Therefore, to reach the precision $\min_{k=0, \dots, K-1} \sum_{i=1}^p \mathbb{E} \left[\|\nabla_i f(X^k)\|_{(i)\star} \right] \leq \epsilon$, it suffices to run the algorithm for

$$K = \left\lceil \frac{\Delta^0}{\phi(\epsilon)} \right\rceil = \left\lceil \frac{2\Delta^0 \sum_{i=1}^p L_i^0}{(1-\zeta)^2 \epsilon^2} + \frac{2\Delta^0 (1+\zeta) L_{\max}^1}{(1-\zeta)^2 \epsilon} \right\rceil$$

iterations.

2. Alternatively, we can start from inequality (22) and apply 4 with $x_i = 1/L_i^1$, $y_i = (1-\zeta) \mathbb{E} \left[\|\nabla_i f(X^k)\|_{(i)\star} \right]$ and $z_i = 2 \left(L_i^0 + (1+\zeta) L_i^1 \mathbb{E} \left[\|\nabla_i f(X^k)\|_{(i)\star} \right] \right)$ to obtain

$$\begin{aligned} \Delta^0 &\geq \sum_{k=0}^{K-1} \sum_{i=1}^p \frac{(1-\zeta)^2 \mathbb{E} \left[\|\nabla_i f(X^k)\|_{(i)\star} \right]^2}{2 \left(L_i^0 + (1+\zeta) L_i^1 \mathbb{E} \left[\|\nabla_i f(X^k)\|_{(i)\star} \right] \right)} \\ &\geq \sum_{k=0}^{K-1} \frac{\left(\sum_{i=1}^p \frac{1}{L_i^1} (1-\zeta) \mathbb{E} \left[\|\nabla_i f(X^k)\|_{(i)\star} \right] \right)^2}{2 \sum_{i=1}^p \left(\frac{L_i^0}{(L_i^1)^2} + (1+\zeta) \frac{1}{L_i^1} \mathbb{E} \left[\|\nabla_i f(X^k)\|_{(i)\star} \right] \right)} \\ &= \sum_{t=0}^{K-1} \psi \left(\sum_{i=1}^p \frac{1}{L_i^1} \mathbb{E} \left[\|\nabla_i f(X^k)\|_{(i)\star} \right] \right), \end{aligned}$$

where $\psi(t) \stackrel{\text{def}}{=} \frac{(1-\zeta)^2 t^2}{2 \left(\sum_{i=1}^p \frac{L_i^0}{(L_i^1)^2} + (1+\zeta) t \right)}$. Since the function ψ is increasing for $t > 0$, ψ^{-1} exists.

It follows that

$$\begin{aligned} \Delta^0 &\geq \sum_{k=0}^{K-1} \psi \left(\sum_{i=1}^p \frac{1}{L_i^1} \mathbb{E} \left[\|\nabla_i f(X^k)\|_{(i)\star} \right] \right) \\ &\geq K \psi \left(\min_{k=0, \dots, K-1} \sum_{i=1}^p \frac{1}{L_i^1} \mathbb{E} \left[\|\nabla_i f(X^k)\|_{(i)\star} \right] \right), \end{aligned}$$

and hence

$$\min_{k=0, \dots, K-1} \sum_{i=1}^p \frac{1}{L_i^1} \mathbb{E} \left[\|\nabla_i f(X^k)\|_{(i)\star} \right] \leq \psi^{-1} \left(\frac{\Delta^0}{K} \right).$$

This in turn means that to reach the precision

$$\min_{k=0, \dots, K-1} \sum_{i=1}^p \left[\frac{\frac{1}{L_i^1}}{\frac{1}{p} \sum_{j=1}^p \frac{1}{L_j^1}} \|\nabla_i f(X^k)\|_{(i)\star} \right] \leq \varepsilon,$$

it suffices to run the algorithm for

$$\begin{aligned}
 K &= \left\lceil \frac{\Delta^0}{\psi \left(\varepsilon \left(\frac{1}{p} \sum_{j=1}^p \frac{1}{L_j^1} \right) \right)} \right\rceil \\
 &= \left\lceil \frac{2\Delta^0 \sum_{i=1}^p \frac{L_i^0}{(L_i^1)^2}}{(1-\zeta)^2 \varepsilon^2 \left(\frac{1}{p} \sum_{j=1}^p \frac{1}{L_j^1} \right)^2} + \frac{2\Delta^0(1+\zeta)}{(1-\zeta)^2 \varepsilon \left(\frac{1}{p} \sum_{j=1}^p \frac{1}{L_j^1} \right)} \right\rceil
 \end{aligned}$$

iterations. ■

F.2. Proof of Theorem 10

We now establish the main result of F. The guarantees in 10 follow from the more general result below.

Theorem 13 *Let Assumptions 1 and 3 hold and fix $\varepsilon > 0$. Let X^0, \dots, X^{K-1} be the iterates of Gluon (Algorithm 2) run with $\beta^k = 1 - (k+1)^{-1/2}$, $t_i^k = t_i(k+1)^{-3/4}$ for some $t_i > 0$, and $M_i^0 = \nabla_i f_{\xi^0}(X^0)$.*

1. If $L_i^1 = 0$, then

$$\begin{aligned}
 &\min_{k=0, \dots, K-1} \sum_{i=1}^p t_i \mathbb{E} \left[\|\nabla_i f(X^k)\|_{(i)\star} \right] \\
 &\leq \frac{\Delta^0}{K^{1/4}} + \frac{1}{K^{1/4}} \sum_{i=1}^p \left[\sigma t_i \left(7 + 2\sqrt{2e^2} \log(K) \right) + L_i^0 t_i^2 \left(\frac{87}{2} + 14 \log(K) \right) \right],
 \end{aligned}$$

2. If $L_i^1 \neq 0$, then for $t_i = \frac{1}{12L_i^1}$, we have

$$\begin{aligned}
 &\min_{k=0, \dots, K-1} \sum_{i=1}^p \frac{1}{12L_i^1} \mathbb{E} \left[\|\nabla_i f(X^k)\|_{(i)\star} \right] \\
 &\leq \frac{2\Delta^0}{K^{1/4}} + \frac{1}{K^{1/4}} \sum_{i=1}^p \left[\frac{\sigma}{6L_i^1} \left(7 + 2\sqrt{2e^2} \log(K) \right) + \frac{L_i^0}{144(L_i^1)^2} (87 + 28 \log(K)) \right],
 \end{aligned}$$

where $\Delta^0 := f(X^0) - \inf_{X \in \mathcal{S}} f(X)$.

Proof We again start with the result in Lemma 2 with $X = X^k$ and $Y = X^{k+1}$, obtaining

$$\begin{aligned}
 f(X^{k+1}) &\leq f(X^k) + \left\langle \nabla f(X^k), X^{k+1} - X^k \right\rangle + \sum_{i=1}^p \frac{L_i^0 + L_i^1 \|\nabla_i f(X^k)\|_{(i)\star}}{2} \|X_i^k - X_i^{k+1}\|_{(i)}^2 \\
 &= f(X^k) + \sum_{i=1}^p \left[\left\langle \nabla_i f(X^k), X_i^{k+1} - X_i^k \right\rangle_{(i)} + \frac{L_i^0 + L_i^1 \|\nabla_i f(X^k)\|_{(i)\star}}{2} \|X_i^k - X_i^{k+1}\|_{(i)}^2 \right] \\
 &= f(X^k) + \sum_{i=1}^p \left[\left\langle M_i^k, X_i^{k+1} - X_i^k \right\rangle_{(i)} + \left\langle \nabla_i f(X^k) - M_i^k, X_i^{k+1} - X_i^k \right\rangle_{(i)} \right] \\
 &\quad + \sum_{i=1}^p \frac{L_i^0 + L_i^1 \|\nabla_i f(X^k)\|_{(i)\star}}{2} \|X_i^k - X_i^{k+1}\|_{(i)}^2.
 \end{aligned}$$

Applying the Cauchy-Schwarz inequality, we have

$$\begin{aligned}
 f(X^{k+1}) &\leq f(X^k) + \sum_{i=1}^p \left[\left\langle M_i^k, X_i^{k+1} - X_i^k \right\rangle_{(i)} + \|\nabla_i f(X^k) - M_i^k\|_{(i)\star} \|X_i^{k+1} - X_i^k\|_{(i)} \right] \\
 &\quad + \sum_{i=1}^p \frac{L_i^0 + L_i^1 \|\nabla_i f(X^k)\|_{(i)\star}}{2} \|X_i^k - X_i^{k+1}\|_{(i)}^2.
 \end{aligned}$$

Now, the update rule (18) and the definition of the dual norm $\|\cdot\|_{(i)\star}$ give

$$\|X_i^k - X_i^{k+1}\|_{(i)}^2 \leq (t_i^k)^2$$

and

$$\left\langle M_i^k, X_i^{k+1} - X_i^k \right\rangle = \left\langle M_i^k, \text{LMO}_{\mathcal{B}_i^k} \left(M_i^k \right) - X_i^k \right\rangle = -t_i^k \max_{\|X_i\|_{(i)} \leq 1} \left\langle M_i^k, X_i \right\rangle = -t_i^k \|M_i^k\|_{(i)\star}.$$

Consequently,

$$\begin{aligned}
 f(X^{k+1}) &\leq f(X^k) + \sum_{i=1}^p \left[-t_i^k \|M_i^k\|_{(i)\star} + t_i^k \|\nabla_i f(X^k) - M_i^k\|_{(i)\star} + \frac{L_i^0 + L_i^1 \|\nabla_i f(X^k)\|_{(i)\star}}{2} (t_i^k)^2 \right] \\
 &= f(X^k) + \sum_{i=1}^p \left[-t_i^k \|M_i^k - \nabla_i f(X^k) + \nabla_i f(X^k)\|_{(i)\star} + t_i^k \|M_i^k - \nabla_i f(X^k)\|_{(i)\star} \right] \\
 &\quad + \sum_{i=1}^p \frac{L_i^0 + L_i^1 \|\nabla_i f(X^k)\|_{(i)\star}}{2} (t_i^k)^2 \\
 &\leq f(X^k) + \sum_{i=1}^p \left[-t_i^k \|\nabla_i f(X^k)\|_{(i)\star} + 2t_i^k \|M_i^k - \nabla_i f(X^k)\|_{(i)\star} \right] \\
 &\quad + \sum_{i=1}^p \frac{L_i^0 + L_i^1 \|\nabla_i f(X^k)\|_{(i)\star}}{2} (t_i^k)^2.
 \end{aligned}$$

Taking expectations, we obtain

$$\begin{aligned} \mathbb{E}[f(X^{k+1})] &\leq \mathbb{E}[f(X^k)] + \sum_{i=1}^p \left[-t_i^k \mathbb{E}[\|\nabla_i f(X^k)\|_{(i)\star}] + 2t_i^k \mathbb{E} \left[\left\| M_i^k - \nabla_i f(X^k) \right\|_{(i)\star} \right] \right. \\ &\quad \left. + \frac{L_i^0 + L_i^1 \mathbb{E}[\|\nabla_i f(X^k)\|_{(i)\star}]}{2} (t_i^k)^2 \right]. \end{aligned}$$

Telescoping the last inequality gives

$$\begin{aligned} \sum_{i=1}^p \sum_{k=0}^{K-1} t_i^k \mathbb{E}[\|\nabla_i f(X^k)\|_{(i)\star}] &\leq \Delta^0 + \sum_{i=1}^p \left[2 \sum_{k=0}^{K-1} t_i^k \mathbb{E} \left[\left\| M_i^k - \nabla_i f(X^k) \right\|_{(i)\star} \right] \right. \\ &\quad \left. + \sum_{k=0}^{K-1} \frac{L_i^0}{2} (t_i^k)^2 + \sum_{k=0}^{K-1} \frac{L_i^1}{2} \mathbb{E}[\|\nabla_i f(X^k)\|_{(i)\star}] (t_i^k)^2 \right], \end{aligned} \quad (24)$$

where $\Delta^0 := f(X^0) - \inf_{X \in \mathcal{S}} f(X)$.

Now, inspired by the analysis in Hübner et al. [11], we introduce the following notation: $\mu_i^k := M_i^k - \nabla_i f(X^k)$, $\gamma_i^k := \nabla_i f_{\xi^k}(X^k) - \nabla_i f(X^k)$, $\alpha^k = 1 - \beta^k$, $\beta^{a:b} := \prod_{k=a}^b \beta^k$ and $S_i^k := \nabla_i f(X^{k-1}) - \nabla_i f(X^k)$. Then, we can rewrite the algorithm's momentum update rule as

$$\begin{aligned} M_i^k &= \beta^k M_i^{k-1} + (1 - \beta^k) \nabla_i f_{\xi^k}(X^k) \\ &= \beta^k \left(\mu_i^{k-1} + \nabla_i f(X^{k-1}) \right) + (1 - \beta^k) \left(\gamma_i^k + \nabla_i f(X^k) \right) \\ &= \nabla_i f(X^k) + \alpha^k \gamma_i^k + \beta^k S_i^k + \beta^k \mu_i^{k-1}. \end{aligned}$$

This yields

$$\begin{aligned} \mu_i^k &= M_i^k - \nabla_i f(X^k) \\ &= \alpha^k \gamma_i^k + \beta^k S_i^k + \beta^k \mu_i^{k-1} \\ &= \sum_{\tau=1}^k \beta^{(\tau+1):k} \alpha^\tau \gamma_i^\tau + \sum_{\tau=1}^k \beta^{\tau:k} S_i^\tau + \beta^{1:k} \mu_i^0 \\ &= \sum_{\tau=0}^k \beta^{(\tau+1):k} \alpha^\tau \gamma_i^\tau + \sum_{\tau=1}^k \beta^{\tau:k} S_i^\tau, \end{aligned}$$

where the last line follows from the fact that $M_i^0 = \nabla_i f_{\xi^0}(X^0)$ and $\beta^0 = 0$. Thus,

$$\begin{aligned} \mathbb{E} \left[\left\| M_i^k - \nabla_i f(X^k) \right\|_{(i)\star} \right] &= \mathbb{E} \left[\left\| \mu_i^k \right\|_{(i)\star} \right] \\ &\leq \mathbb{E} \left[\left\| \sum_{\tau=0}^k \beta^{(\tau+1):k} \alpha^\tau \gamma_i^\tau \right\|_{(i)\star} \right] + \sum_{\tau=1}^k \beta^{\tau:k} \mathbb{E} \left[\left\| S_i^\tau \right\|_{(i)\star} \right] \\ &= \sqrt{\sum_{\tau=0}^k (\beta^{(\tau+1):k} \alpha^\tau)^2 \mathbb{E} \left[\left\| \gamma_i^\tau \right\|_{(i)\star}^2 \right]} + \sum_{\tau=1}^k \beta^{\tau:k} \mathbb{E} \left[\left\| S_i^\tau \right\|_{(i)\star} \right], \end{aligned}$$

where in the last equality we used the fact that for all $q < l$

$$\begin{aligned}\mathbb{E} \left[(\gamma_i^l)^\top \gamma_i^q \right] &= \mathbb{E} \left[\mathbb{E} \left[(\gamma_i^l)^\top \gamma_i^q \mid X_i^l \right] \right] = \mathbb{E} \left[\mathbb{E} \left[\gamma_i^l \mid X_i^l \right]^\top \gamma_i^q \right] \\ &= \mathbb{E} \left[\left(\mathbb{E} \left[\nabla_i f_{\xi^l}(X^l) - \nabla_i f(X^l) \mid X_i^l \right] \right)^\top \gamma_i^q \right] = 0,\end{aligned}$$

Using Assumptions 1 and 3, we get

$$\mathbb{E} \left[\|\gamma_i^\tau\|_{(i)\star}^2 \right] = \mathbb{E} \left[\underbrace{\mathbb{E} \left[\|\gamma_i^\tau\|_{(i)\star}^2 \mid X_i^\tau \right]}_{\leq \sigma^2} \right] \leq \sigma^2$$

and

$$\|S_i^\tau\|_{(i)\star} \leq (L_i^0 + L_i^1 \|\nabla_i f(X^\tau)\|_{(i)\star}) \|X_i^{\tau+1} - X_i^\tau\|_{(i)} \leq (L_i^0 + L_i^1 \|\nabla_i f(X^\tau)\|_{(i)\star}) t_i^\tau.$$

Therefore,

$$\begin{aligned}\mathbb{E} \left[\|M_i^k - \nabla_i f(X^k)\|_{(i)\star} \right] &\leq \sigma \sqrt{\sum_{\tau=0}^k (\beta^{(\tau+1):k} \alpha^\tau)^2} + L_i^0 \sum_{\tau=1}^k \beta^{\tau:k} t_i^\tau \\ &\quad + L_i^1 \sum_{\tau=1}^k \beta^{\tau:k} t_i^\tau \mathbb{E} \left[\|\nabla_i f(X^\tau)\|_{(i)\star} \right].\end{aligned}$$

Combining the last inequality with (24) gives

$$\begin{aligned}\sum_{i=1}^p \sum_{k=0}^{K-1} t_i^k \mathbb{E} \left[\|\nabla_i f(X^k)\|_{(i)\star} \right] &\leq \Delta^0 + \sum_{i=1}^p \left[\underbrace{2\sigma \sum_{k=0}^{K-1} t_i^k \sqrt{\sum_{\tau=0}^k (\beta^{(\tau+1):k} \alpha^\tau)^2}}_{=: I_1} + \underbrace{2L_i^0 \sum_{k=0}^{K-1} t_i^k \sum_{\tau=1}^k \beta^{\tau:k} t_i^\tau}_{=: I_2} \right. \\ &\quad \left. + \underbrace{2L_i^1 \sum_{k=0}^{K-1} t_i^k \sum_{\tau=1}^k \beta^{\tau:k} t_i^\tau \mathbb{E} \left[\|\nabla_i f(X^\tau)\|_{(i)\star} \right]}_{=: I_3} \right. \\ &\quad \left. + \underbrace{\frac{L_i^0}{2} \sum_{k=0}^{K-1} (t_i^k)^2 + \frac{L_i^1}{2} \sum_{k=0}^{K-1} (t_i^k)^2 \mathbb{E} \left[\|\nabla_i f(X^k)\|_{(i)\star} \right]}_{=: I_4} \right].\end{aligned}\tag{25}$$

Let us now upper-bound each term I_i , $i = 1, 2, 3, 4$.

I_1 : using Lemma 6, we obtain

$$I_1 \leq \sigma t_i \left(7 + 2\sqrt{2e^2} \log(K) \right).$$

I_2 : using Lemma 6, we obtain

$$I_2 \leq 14L_i^0 t_i^2 (3 + \log(K)).$$

I_3 : rearranging the sums and using Lemma 5 with $a = \tau + 1, b = K, p = 3/4$ and $q = 1/2$, we have

$$\begin{aligned} I_3 &= 2L_i^1 \sum_{k=0}^{K-1} t_i^k \sum_{\tau=1}^k \beta^{\tau:k} t_i^\tau \mathbb{E} [\|\nabla_i f(X^\tau)\|_{(i)\star}] \\ &= 2L_i^1 \sum_{\tau=1}^{K-1} t_i^\tau \left(\sum_{k=\tau}^{K-1} t_i^k \beta^{\tau:k} \right) \mathbb{E} [\|\nabla_i f(X^\tau)\|_{(i)\star}] \\ &= 2L_i^1 \sum_{\tau=1}^{K-1} t_i^\tau t_i \left(\sum_{k=\tau}^{K-1} (k+1)^{-3/4} \beta^{\tau:k} \right) \mathbb{E} [\|\nabla_i f(X^\tau)\|_{(i)\star}] \\ &\leq 2L_i^1 \sum_{\tau=1}^{K-1} t_i^\tau t_i \tau^{-1/4} \underbrace{e^{2((\tau+1)^{1/2} - \tau^{1/2})}}_{\leq e^{2(\sqrt{2}-1)} \text{ for } \tau \geq 1} \mathbb{E} [\|\nabla_i f(X^\tau)\|_{(i)\star}] \\ &\leq 2e^{2(\sqrt{2}-1)} L_i^1 \sum_{\tau=1}^{K-1} t_i^\tau t_i \tau^{-1/4} \mathbb{E} [\|\nabla_i f(X^\tau)\|_{(i)\star}] \\ &\leq 2e^{2(\sqrt{2}-1)} L_i^1 \sum_{k=0}^{K-1} t_i^k t_i \mathbb{E} [\|\nabla_i f(X^k)\|_{(i)\star}]. \end{aligned}$$

I_4 :

$$\begin{aligned} I_4 &= \frac{L_i^0}{2} \sum_{k=0}^{K-1} \left(t_i^k \right)^2 \leq \frac{L_i^0}{2} \sum_{k=0}^{\infty} \left(t_i^k \right)^2 = \frac{L_i^0}{2} t_i^2 \sum_{k=0}^{\infty} (1+k)^{-3/2} \\ &\leq \frac{L_i^0}{2} t_i^2 \left(1 + \int_1^{\infty} \frac{1}{z^{3/2}} dz \right) = \frac{3L_i^0}{2} t_i^2. \end{aligned}$$

Combining the upper-bounds for $I_i, i = 1, 2, 3, 4$ with (25) gives

$$\begin{aligned} \sum_{i=1}^p \sum_{k=0}^{K-1} t_i^k \mathbb{E} [\|\nabla_i f(X^k)\|_{(i)\star}] &\leq \Delta^0 + \sum_{i=1}^p \left[\sigma t_i \left(7 + 2\sqrt{2e^2} \log(K) \right) + 14L_i^0 t_i^2 (3 + \log(K)) \right. \\ &\quad \left. + 2e^{2(\sqrt{2}-1)} L_i^1 \sum_{k=0}^{K-1} t_i^k t_i \mathbb{E} [\|\nabla_i f(X^k)\|_{(i)\star}] \right. \\ &\quad \left. + \frac{3L_i^0}{2} t_i^2 + \frac{L_i^1}{2} \sum_{k=0}^{K-1} \left(t_i^k \right)^2 \mathbb{E} [\|\nabla_i f(X^k)\|_{(i)\star}] \right]. \end{aligned}$$

Using the fact that $t_i^k = t_i(1+k)^{-3/4} \leq t_i$, and denoting $C := 2e^{2(\sqrt{2}-1)} + \frac{1}{2} \leq 5.1$, we get

$$\begin{aligned} \sum_{i=1}^p \sum_{k=0}^{K-1} t_i^k \mathbb{E}[\|\nabla_i f(X^k)\|_{(i)\star}] &\leq \Delta^0 + \sum_{i=1}^p \left[\sigma t_i \left(7 + 2\sqrt{2e^2} \log(K) \right) + 14L_i^0 t_i^2 \left(\frac{87}{28} + \log(K) \right) \right. \\ &\quad \left. + CL_i^1 t_i \sum_{k=0}^{K-1} t_i^k \mathbb{E} \left[\|\nabla_i f(X^k)\|_{(i)\star} \right] \right]. \end{aligned}$$

Now, let us consider two options: (1) $L_i^1 = 0$ for all $i \in \{1, \dots, p\}$ and (2) $L_i^1 \neq 0$, for all $i \in \{1, \dots, p\}$.

Case 1: $L_i^1 = 0, i = 1, \dots, p$. In this case,

$$\sum_{i=1}^p \sum_{k=0}^{K-1} t_i^k \mathbb{E}[\|\nabla_i f(X^k)\|_{(i)\star}] \leq \Delta^0 + \sum_{i=1}^p \left[\sigma t_i \left(7 + 2\sqrt{2e^2} \log(K) \right) + 14L_i^0 t_i^2 \left(\frac{87}{28} + \log(K) \right) \right],$$

and therefore,

$$\begin{aligned} &\min_{k=0, \dots, K-1} \sum_{i=1}^p t_i \mathbb{E}[\|\nabla_i f(X^k)\|_{(i)\star}] \\ &\leq \frac{1}{K} \sum_{k=0}^{K-1} \sum_{i=1}^p t_i \mathbb{E}[\|\nabla_i f(X^k)\|_{(i)\star}] \\ &\leq \frac{1}{K^{1/4}} \sum_{k=0}^{K-1} \sum_{i=1}^p t_i (1+k)^{-3/4} \mathbb{E}[\|\nabla_i f(X^k)\|_{(i)\star}] \\ &= \frac{1}{K^{1/4}} \sum_{k=0}^{K-1} \sum_{i=1}^p t_i^k \mathbb{E}[\|\nabla_i f(X^k)\|_{(i)\star}] \\ &\leq \frac{\Delta^0}{K^{1/4}} + \frac{1}{K^{1/4}} \sum_{i=1}^p \left[\sigma t_i \left(7 + 2\sqrt{2e^2} \log(K) \right) + L_i^0 t_i^2 \left(\frac{87}{2} + 14 \log(K) \right) \right]. \end{aligned}$$

Case 2: $L_i^1 \neq 0, i = 1, \dots, p$. Let us choose $t_i = \frac{1}{12L_i^1}$. Then

$$\sum_{i=1}^p \sum_{k=0}^{K-1} t_i^k \mathbb{E}[\|\nabla_i f(X^k)\|_{(i)\star}] \leq 2\Delta^0 + \sum_{i=1}^p \left[2\sigma t_i \left(7 + 2\sqrt{2e^2} \log(K) \right) + L_i^0 t_i^2 (87 + 28 \log(K)) \right],$$

and hence

$$\begin{aligned}
 & \min_{k=0, \dots, K-1} \sum_{i=1}^p \frac{1}{12L_i^1} \mathbb{E}[\|\nabla_i f(X^k)\|_{(i)\star}] \\
 & \leq \frac{1}{K} \sum_{k=0}^{K-1} \sum_{i=1}^p t_i \mathbb{E}[\|\nabla_i f(X^k)\|_{(i)\star}] \\
 & \leq \frac{1}{K^{1/4}} \sum_{k=0}^{K-1} \sum_{i=1}^p t_i (1+k)^{-3/4} \mathbb{E}[\|\nabla_i f(X^k)\|_{(i)\star}] \\
 & = \frac{1}{K^{1/4}} \sum_{i=1}^p \sum_{k=0}^{K-1} t_i^k \mathbb{E}[\|\nabla_i f(X^k)\|_{(i)\star}] \\
 & \leq \frac{2\Delta^0}{K^{1/4}} + \frac{1}{K^{1/4}} \sum_{i=1}^p \left[\frac{\sigma}{6L_i^1} \left(7 + 2\sqrt{2e^2} \log(K) \right) + \frac{L_i^0}{144(L_i^1)^2} (87 + 28 \log(K)) \right].
 \end{aligned}$$

■

Appendix G. Additional experimental results and details

G.1. Experimental details

All experiments for the NanoGPT model are conducted using PyTorch⁵ with Distributed Data Parallel (DDP)⁶ across 4 NVIDIA A100 GPUs (40GB each). For the CNN experiments, training is performed on a single NVIDIA A100 GPU (40GB). The training and evaluation pipelines are implemented using open-source codebases [14, 15, 28], with all modifications clearly documented and properly referenced where applicable.

For LMO-based methods, we compute inexact LMOs using the Newton–Schulz iteration when an analytical solution is unavailable (e.g., for SVD-type updates), following the approach proposed by Jordan et al. [16]. This method provides a computationally efficient approximation of the required orthogonalization while preserving the convergence behavior of the overall algorithm.

G.2. Fitting L_i^0 and L_i^1

To minimize the Euclidean error between the true value $\hat{L}_i[k]$ and its approximation $\hat{L}_i^{\text{approx}}[k]$, while penalizing underestimation, we incorporate a hinge-like penalty term. Specifically, we fit L_i^0 and L_i^1 by minimizing the loss function

$$\mathcal{L}_i(L_i^0, L_i^1) := \sum_{k=0}^{K-1} \left(\hat{L}_i[k] - \hat{L}_i^{\text{approx}}[k] \right)^2 + \lambda \sum_{k=0}^{K-1} \max \left(0, \hat{L}_i[k] - \hat{L}_i^{\text{approx}}[k] \right)^2. \quad (26)$$

The first term of \mathcal{L}_i captures the standard Euclidean (squared) error, while the second term introduces an additional penalty proportional to the amount of underestimation (i.e., when $\hat{L}_i[k] > \hat{L}_i^{\text{approx}}[k]$). The hyperparameter $\lambda \geq 0$ controls the strength of this penalty.

G.3. Training NanoGPT on FineWeb.

In this section, we present additional results and experimental details for the experiment described in the main text, which involves training a NanoGPT model on the FineWeb dataset using the unScion optimizer.

Below, we highlight selected experimental results for the unScion optimizer, a special case of Gluon (see E.1).

G.3.1. EXPERIMENTAL SETUP

In the first set of experiments, we aim to verify layer-wise (L^0, L^1) -smoothness (1). To this end, we train the NanoGPT model with 124M parameters on the FineWeb dataset, leveraging two open-source GitHub repositories [15, 28]. We use the unScion optimizer, i.e., Gluon with the norm choices as in (9). We adopt the hyperparameters from Pethick et al. [29, Table 7], mapping their values $\gamma = 0.00036$, $\rho_2 = 50$, and $\rho_3 = 3000$ into our notation as follows: $t_i^k \equiv \gamma \rho_2 = 0.018$ for $i = 1, \dots, p-1$ (corresponding to the transformer block layers), and $t_p^k \equiv \gamma \rho_3 = 1.08$ (token

5. PyTorch Documentation. Available at: <https://pytorch.org/docs/stable/index.html>

6. Distributed Data Parallel (DDP) in PyTorch. Available at: <https://pytorch.org/docs/stable/notes/ddp.html>

embeddings and output projections, due to weight sharing). We set the number of warmdown iterations to 0 to keep the learning rates constant throughout training. The model is trained for 5,000 iterations in accordance with the Chinchilla scaling laws to ensure compute-optimal training.

G.3.2. THEORETICAL STEPSIZE PREDICTION

Based on the estimated values of L_i^0 and L_i^1 , assuming that 1 holds and ignoring gradient stochasticity, 1 suggests the stepsizes

$$\begin{aligned} t_i^k &= \frac{\|\nabla_i f_{\xi^k}(X^k)\|_{(i)\star}}{L_i^0 + L_i^1 \|\nabla_i f_{\xi^k}(X^k)\|_{(i)\star}} \approx \frac{1}{L_i^1} \approx \frac{1}{70} \approx 0.014, \quad i = 1, \dots, p-1, \\ t_p^k &= \frac{\|\nabla_p f_{\xi^k}(X^k)\|_{(p)\star}}{L_p^0 + L_p^1 \|\nabla_p f_{\xi^k}(X^k)\|_{(p)\star}} \approx \frac{1}{L_p^1} \approx \frac{1}{1.3} \approx 0.77. \end{aligned} \quad (27)$$

Remarkably, these values align closely with the manually tuned values reported earlier, again underscoring the predictive power of our theoretical prescriptions (see 3).

G.3.3. EMPIRICAL VALIDATION OF 1

We begin by presenting additional results for the experiment described in 4, aimed at empirically validating 1. We plot the estimated *trajectory smoothness*

$$\hat{L}_i[k] \stackrel{\text{def}}{=} \frac{\|\nabla_i f_{\xi^{k+1}}(X^{k+1}) - \nabla_i f_{\xi^k}(X^k)\|_{(i)\star}}{\|X_i^{k+1} - X_i^k\|_{(i)}} \quad (28)$$

and its approximation

$$\hat{L}_i^{\text{approx}}[k] \stackrel{\text{def}}{=} L_i^0 + L_i^1 \|\nabla_i f_{\xi^{k+1}}(X^{k+1})\|_{(i)\star} \quad (29)$$

as functions of the iteration index k , where $L_i^0, L_i^1 \geq 0$ are fitted using the procedure described in G.2.

Figures 5, 6, and 7 show results for parameter groups from the embedding layer and from the 4th and 8th transformer blocks. Similar patterns are observed across all layers. In each case, we see a strong agreement between $\hat{L}_i[k]$ and $\hat{L}_i^{\text{approx}}[k]$, suggesting that 1 holds approximately along the optimization trajectory.

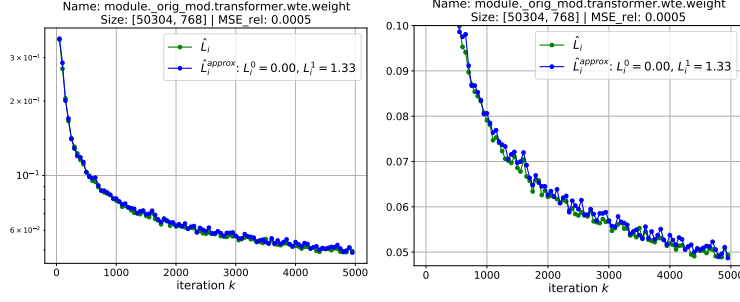


Figure 5: Validation of layer-wise (L^0, L^1) -smoothness for the group of parameters from the embedding layer of NanoGPT-124M along unScion training trajectories. The group norm is $\|\cdot\|_{(p)} = n_p \|\cdot\|_{1 \rightarrow \infty}$, with fitted values $L_p^0 \approx 0$, $L_p^1 \approx 1.33$. The same plot is shown twice with different y -axis limits.

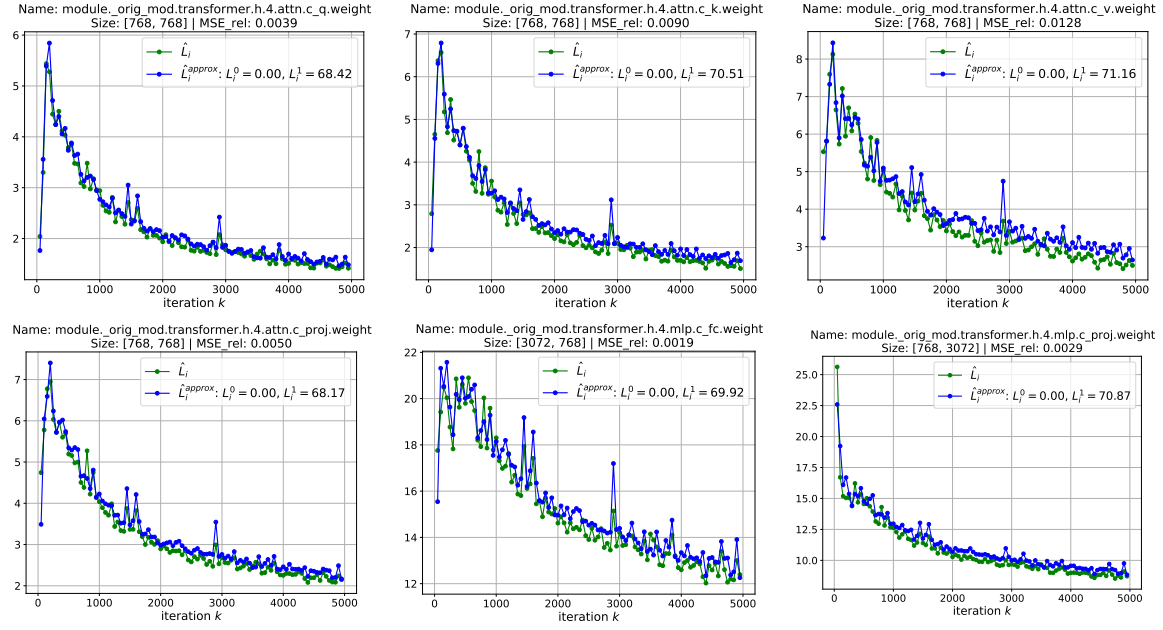


Figure 6: Validation of layer-wise (L^0, L^1) -smoothness for the group of parameters from the 4th transformer block of NanoGPT-124M along unScion training trajectories. The group norms are $\|\cdot\|_{(i)} = \sqrt{n_i/m_i} \|\cdot\|_{2 \rightarrow 2}$, with fitted values $L_i^0 \approx 0$, $L_i^1 \approx 70$.

G.3.4. GENERALIZED SMOOTHNESS UNDER EUCLIDEAN VS. SPECIALIZED NORMS

In this experiment, we compare how well the layer-wise (L^0, L^1) -smoothness assumption is satisfied under the standard Euclidean norms $\|\cdot\|_2$ for each parameter block, as opposed to the specialized norms described in (9). We adopt the same training setup as in Section 4, plotting the estimated trajectory smoothness \hat{L}_i and its approximation $\hat{L}_i^{\text{approx}}$ along the training trajectories across several parameter groups. Unlike previous sections, here we do not penalize instances where $\hat{L}_i > \hat{L}_i^{\text{approx}}$ in order to find the best approximation (i.e., $\lambda = 0$ in (26)). Additionally, when using the standard Euclidean norm $\|\cdot\|_2$ for approximation, we exclude the first point, as it could distort the result.

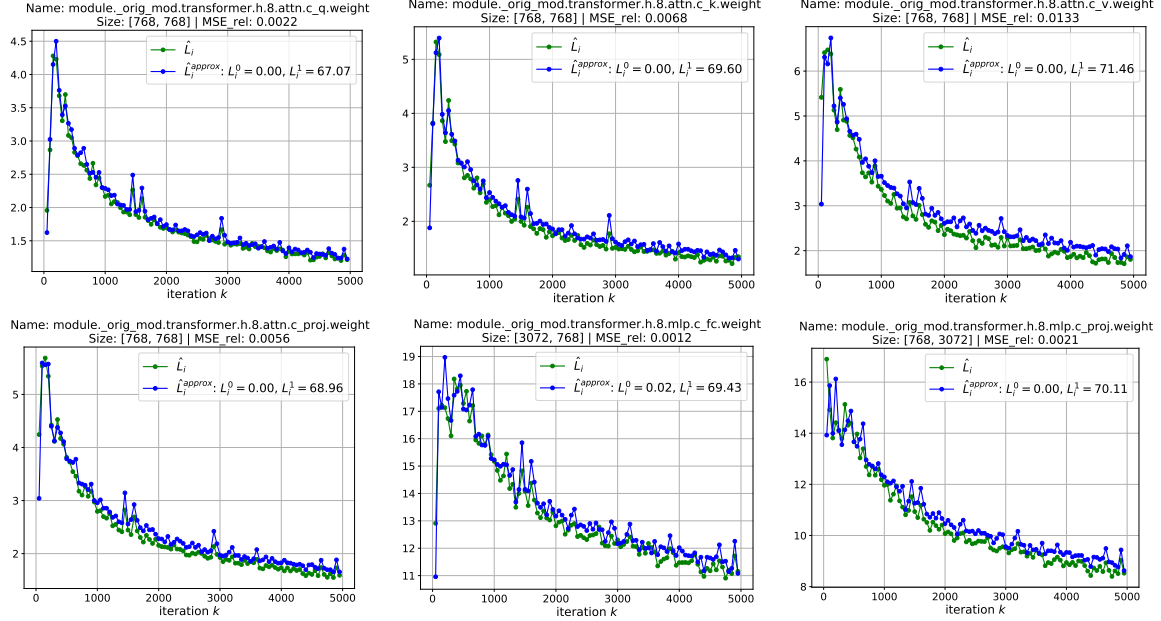


Figure 7: Validation of layer-wise (L^0, L^1) -smoothness for the group of parameters from the 8th transformer block of NanoGPT-124M along unScion training trajectories. The group norms are $\|\cdot\|_{(i)} = \sqrt{n_i/m_i} \|\cdot\|_{2 \rightarrow 2}$, with fitted values $L_i^0 \approx 0, L_i^1 \approx 70$.

We evaluate the quality of each approximation using the relative mean squared error ($\text{MSE}_i^{\text{rel}}$, denoted MSE_{rel} in the figures), defined as

$$\text{MSE}_i^{\text{rel}} := \frac{1}{K} \sum_{i=1}^K \left(\frac{\hat{L}_i[k] - \hat{L}_i^{\text{approx}}[k]}{\hat{L}_i[k]} \right)^2,$$

where a lower value indicates a better fit.

As shown in Figures 14 and 21, both visually and in terms of $\text{MSE}_i^{\text{rel}}$, using specialized norms for each group of parameters provides a better approximation than the standard Euclidean norm $\|\cdot\|_2$. Notably, the relative mean squared error $\text{MSE}_i^{\text{rel}}$ is consistently an order of magnitude lower under specialized norms.

G.3.5. LEARNING RATE TRANSFER FROM ADAMW

We now aim to verify layer-wise (L^0, L^1) -smoothness following the approach used in Section 4, but employing the AdamW optimizer. We use hyperparameters specified in Pethick et al. [29, Table 7]. In Figure 22, we present the results for the estimated trajectory smoothness \hat{L}_i and its approximation $\hat{L}_i^{\text{approx}}$ across several parameter groups along the training trajectories. Notably, for the group of parameters from the embedding layer X_p (the last plot in Figure 22), the fitted value of L_p^1 is approximately 20–30 times smaller than in other groups. Since in all plots we observe that $L_i^0 \ll L_i^1 \|\nabla_i f_{\xi^k}(X^k)\|_{(i)*}$, 1 implies that $t_i^k \approx 1/L_i^k$. Thus, t_p^k should be 20–30 times larger than t_i^k for $i = 1, \dots, p-1$, which is consistent with the tuned parameters from Pethick et al. [29, Table 7].

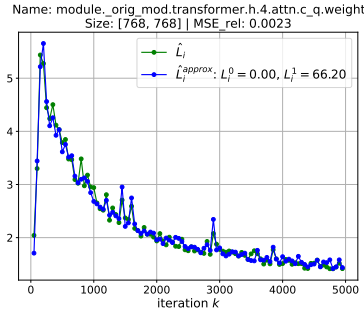
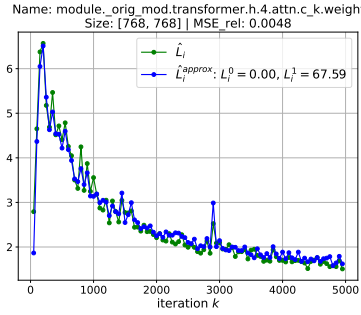
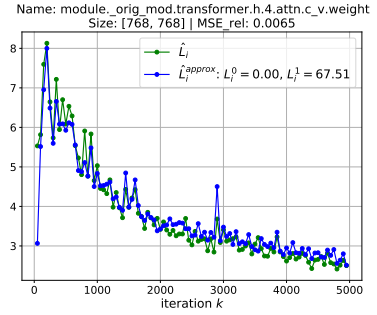
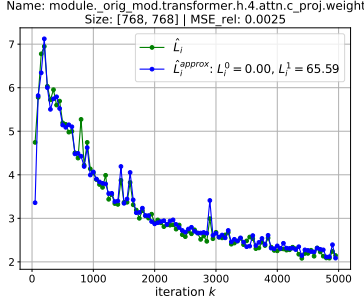
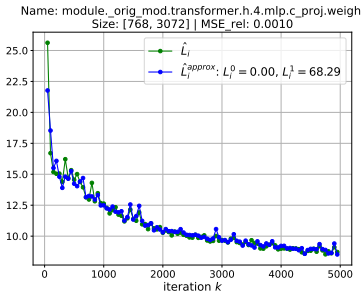
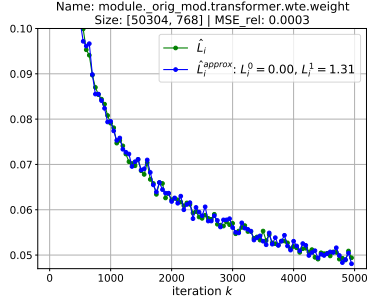

 Figure 8: $MSE_i^{\text{rel}} = 0.0023$

 Figure 9: $MSE_i^{\text{rel}} = 0.0048$

 Figure 10: $MSE_i^{\text{rel}} = 0.0065$

 Figure 11: $MSE_i^{\text{rel}} = 0.0025$

 Figure 12: $MSE_i^{\text{rel}} = 0.001$

 Figure 13: $MSE_i^{\text{rel}} = 0.0003$

 Figure 14: Validation of layer-wise (L^0, L^1) -smoothness for different groups of parameters in NanoGPT-12.4M along training trajectories of unScion using the specialized norm choices defined in (9).

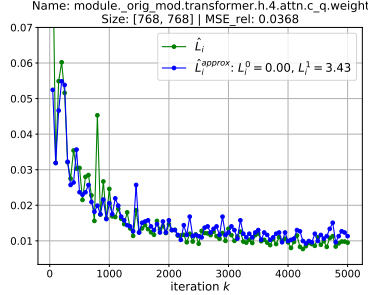
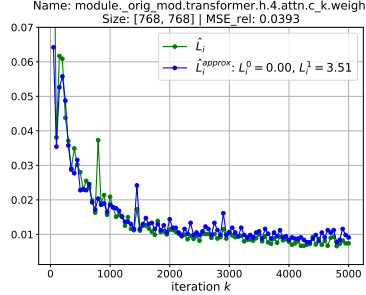
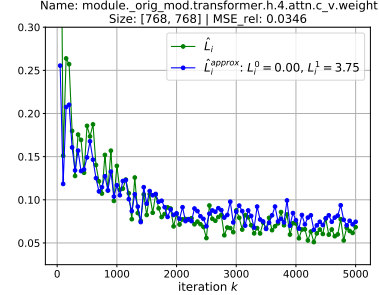
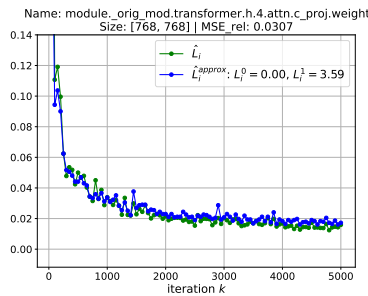
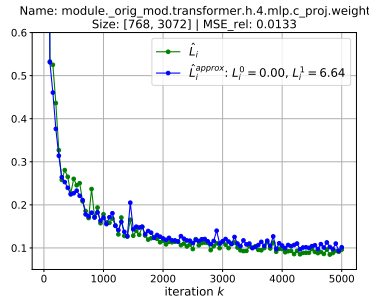
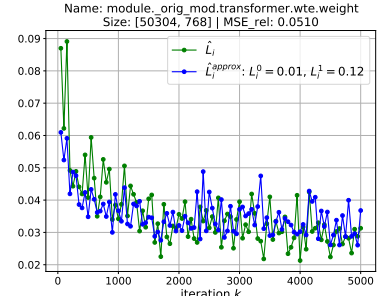
This insight provides an efficient and principled method for initializing learning rates in **Scion**. Smoothness statistics collected during standard **AdamW** training (which is commonly used for training LLMs) can serve as a strong prior, allowing practitioners to directly incorporate structure-aware choices, such as larger stepsizes for embedding layers, into their tuning process. Importantly, computing these statistics is computationally inexpensive, introducing minimal additional cost.

G.3.6. ABLATION STUDY ON LEARNING RATE SCALING FACTORS

We next evaluate the impact of the learning rate scaling factors ρ_2 and ρ_3 on the performance of the **unScion** optimizer. For consistency, all other hyperparameters are fixed as described earlier. As a baseline, we include results obtained with the **AdamW** optimizer, using the hyperparameter settings from Section G.3.5. 25 presents (a) validation curves for both optimizers, with varying ρ_3 in **unScion**, and (b) the final validation loss for **unScion** across different combinations of ρ_2 and ρ_3 . The best performance is achieved with $\rho_2 = 50$ and $\rho_3 = 3000$, i.e., $t_i^k = 0.018$ for $i = 1, \dots, p-1$ and $t_p^k = 1.08$, consistent with our theoretical prediction from 1 (which suggests $t_i^k \approx \frac{1}{L_i^1}$ when $L_i^0 \approx 0$). This supports the use of non-uniform scaling across layers, with larger stepsizes for the embedding layer.

G.4. Training CNN on CIFAR-10

In this experiment, we further validate layer-wise (L^0, L^1) -smoothness by training a CNN model on the CIFAR-10 dataset, following implementations from two open-source GitHub repositories [14, 28]. The model is trained using the **unScion** optimizer (10) with full-batch gradients $\nabla_i f$, no

Figure 15: $MSE_i^{\text{rel}} = 0.0368$ Figure 16: $MSE_i^{\text{rel}} = 0.0393$ Figure 17: $MSE_i^{\text{rel}} = 0.0346$ Figure 18: $MSE_i^{\text{rel}} = 0.0307$ Figure 19: $MSE_i^{\text{rel}} = 0.0133$ Figure 20: $MSE_i^{\text{rel}} = 0.051$ Figure 21: Validation of layer-wise (L^0, L^1) -smoothness for different groups of parameters in NanoGPT-124M along training trajectories of `unScion` using the standard Euclidean norm $\|\cdot\|_2$.

momentum and no learning rate decay (results for the stochastic case are reported below). Other hyperparameters are as in Pethick et al. [29, Table10], except that we train for more epochs.

Similar to the NanoGPT experiments discussed in 4, we plot the estimated (non-stochastic) trajectory smoothness $\hat{L}_i[k] \stackrel{\text{def}}{=} \|\nabla_i f(X^{k+1}) - \nabla_i f(X^k)\|_{(i)\star} / \|X_i^{k+1} - X_i^k\|_{(i)}$ alongside its approximation $\hat{L}_i^{\text{approx}}[k] \stackrel{\text{def}}{=} L_i^0 + L_i^1 \|\nabla_i f(X^{k+1})\|_{(i)\star}$ for selected parameter groups. In this experiment, we consider a simplified variant of 1, setting $L_i^0 = 0$, and estimate $L_i^1 \geq 0$ using the same procedure as in 4.

Figure 26 presents the results, demonstrating that 1 is approximately satisfied along the training trajectory. When this condition holds with $L_i^0 = 0$, 1 guarantees convergence under the stepsize choice $t_i^k \equiv t_i = 1/L_i^1$. In this setting, the estimated L_i^1 values (shown in Figure 26) are $L_i^1 \approx 3$ for all parameter groups except for the classification head weights X_p , where $L_p^1 \approx 0.03$. This roughly two-orders-of-magnitude difference justifies the much larger radius t_p^k used for the head weights in the tuned configuration reported in Pethick et al. [29, Table 10].

In this section, we provide additional results for the experiments described above, where a CNN model is trained on the CIFAR-10 dataset using the `unScion` optimizer.

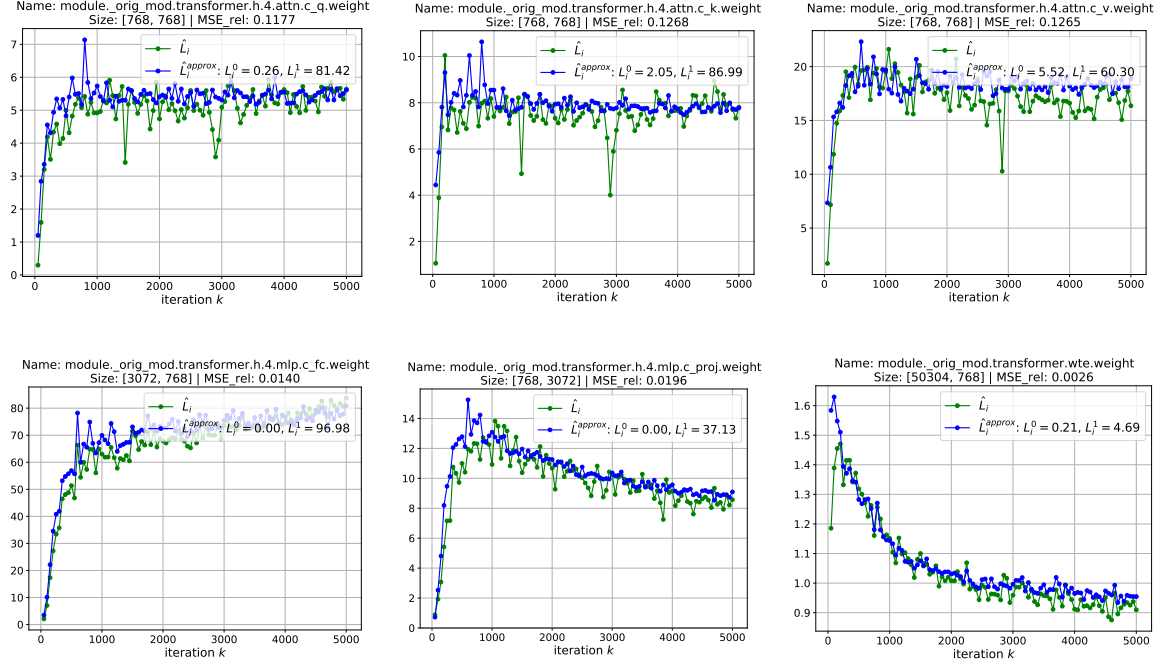


Figure 22: Validation of layer-wise (L^0, L^1) -smoothness for different groups of parameters in NanoGPT-124M along AdamW training trajectories.

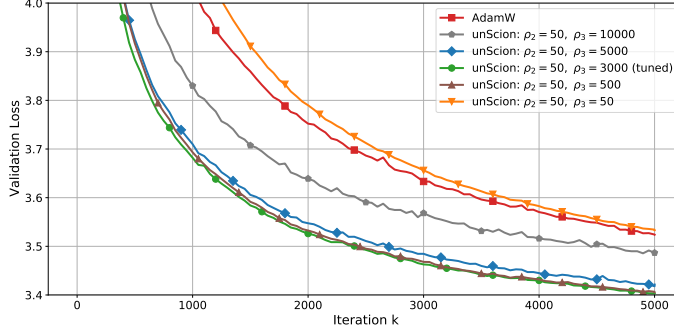


Figure 23

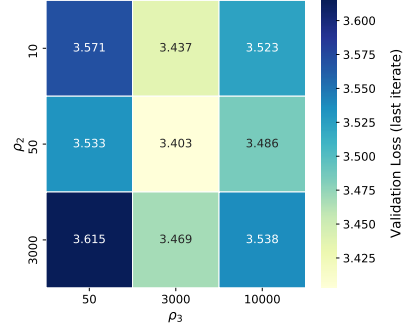


Figure 24

Figure 25: (a) Validation curves for AdamW and unScion with varying ρ_3 values; (b) Heatmap of validation loss from the last iteration of unScion across different combinations of ρ_2 and ρ_3 .

Full-batch (deterministic) gradients. We begin with presenting additional results in the deterministic setting. Figure 26 shows the estimated trajectory smoothness

$$\hat{L}_i[k] \stackrel{\text{def}}{=} \frac{\|\nabla_i f(X^{k+1}) - \nabla_i f(X^k)\|_{(i)\star}}{\|X_i^{k+1} - X_i^k\|_{(i)}}$$

and its approximation

$$\hat{L}_i^{\text{approx}}[k] \stackrel{\text{def}}{=} L_i^1 \|\nabla_i f(X^{k+1})\|_{(i)\star}$$

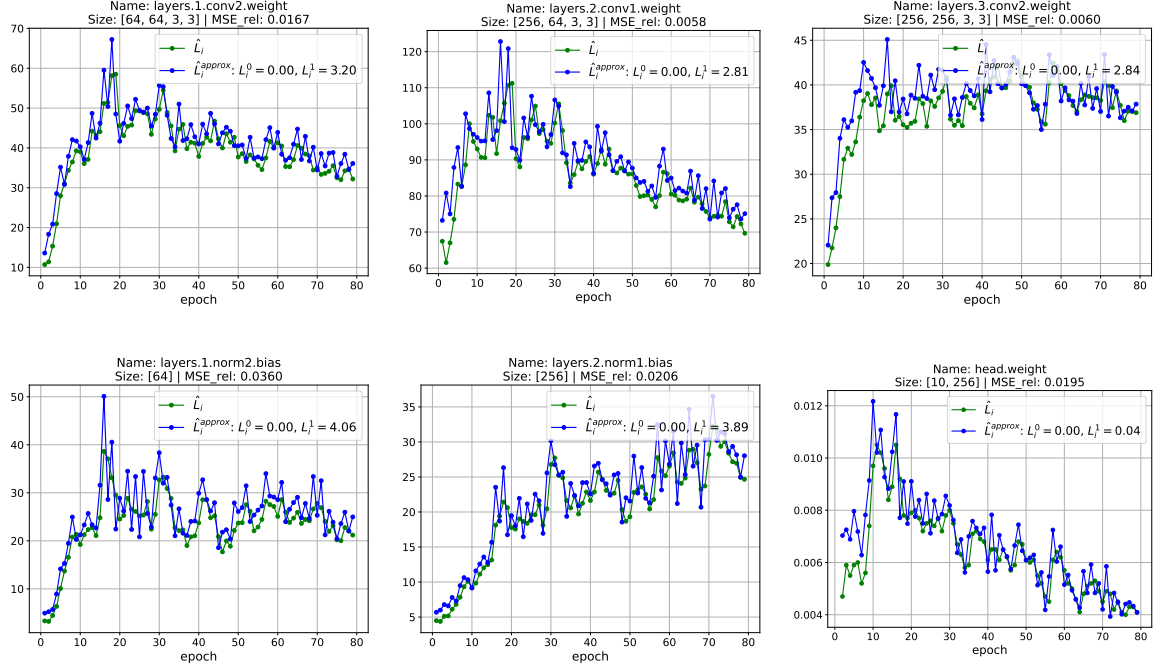


Figure 26: Validation of layer-wise (L^0, L^1) -smoothness for different groups of parameters of a CNN model along the training trajectories of **unScion** with **full-batch gradients**. The norms used for each group are as follows: $\|\cdot\|_{(i)} = \sqrt{1/C_i^{out}} \|\cdot\|_2$ for biases, $\|\cdot\|_{(i)} = k^2 \sqrt{C_i^{in}/C_i^{out}} \|\cdot\|_{2 \rightarrow 2}$ for conv, and $\|\cdot\|_{(p)} = n_p \|\cdot\|_{1 \rightarrow \infty}$ for the last group X_p , associated with classification head weights.

(where we set $L_i^0 = 0$) for a broader selection of parameter groups than shown in the main text. The results further support the validity of Assumption 1 with $L_i^0 = 0$.

Stochastic gradients.

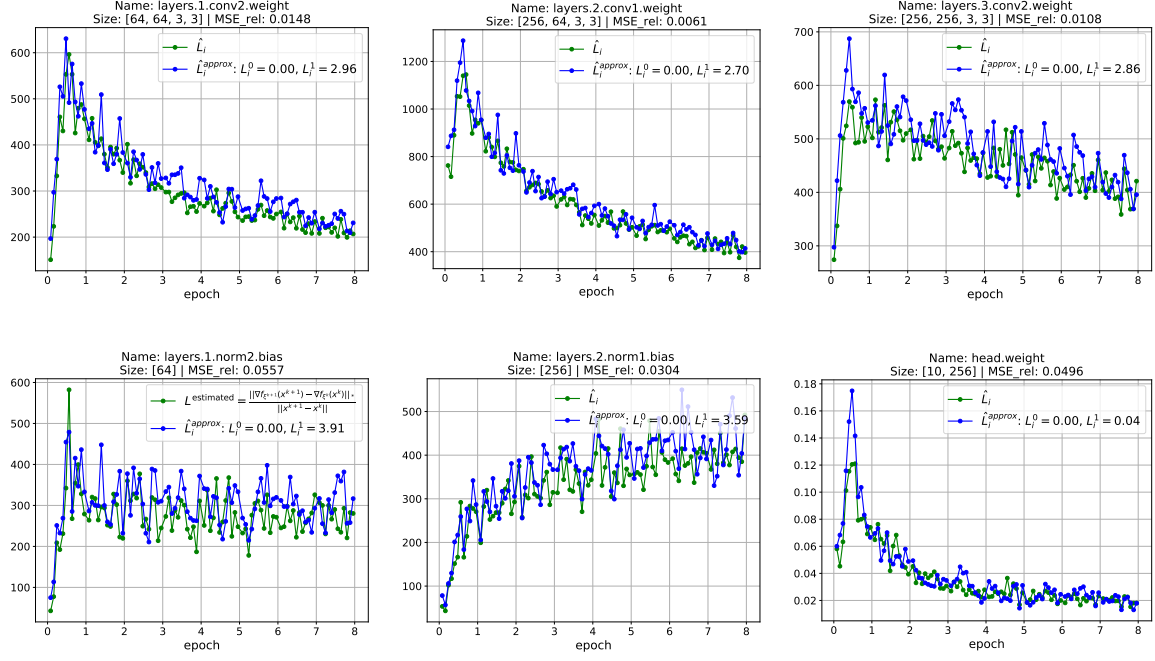


Figure 27: Validation of layer-wise (L^0, L^1) -smoothness for different groups of parameters of a CNN model along the training trajectories of **unScion** with **stochastic gradients**. The norms used for each group are as follows: $\|\cdot\|_{(i)} = \sqrt{1/C_i^{out}} \|\cdot\|_2$ for biases, $\|\cdot\|_{(i)} = k^2 \sqrt{C_i^{in}/C_i^{out}} \|\cdot\|_{2 \rightarrow 2}$ for conv, and $\|\cdot\|_{(p)} = n_p \|\cdot\|_{1 \rightarrow \infty}$ for the last group X_p , associated with classification head weights.

Appendix H. Conclusion and future work

In this work, we propose **Gluon**, an LMO-based optimization method that recovers state-of-the-art optimizers such as **Muon** and **Scion** as special cases. We develop a principled analytical framework for layer-wise optimization based on a novel *layer-wise* (L^0, L^1) -smoothness assumption, which captures the anisotropic structure of modern deep networks. This assumption enables sharper and more general convergence guarantees and, unlike prior analyses, yields theoretical stepsizes that closely match those found via finetuning. Our framework thus provides *the first rigorous and practically predictive analysis of modern layer-wise optimizers*. Experiments confirm that the assumption holds approximately throughout training, reinforcing its practical relevance. Together, these results offer a refined foundation for structured optimization in deep learning.

While this work resolves two key theoretical gaps (Sections 2.1 and 2.2), it also highlights important directions for future research. Our analysis assumes exact LMO computations, whereas practical implementations use approximations (G.1). Additionally, our stochastic guarantees (10) rely on the widely adopted bounded variance assumption, which may not hold in certain scenarios, e.g., under subsampling [18]. Finally, our support for adaptive stepsizes is currently restricted to the deterministic setting. While they also perform well empirically in the stochastic regime (4), a complete theoretical justification remains an open challenge.

In summary, although we make substantial progress by closing the two most critical gaps—establishing a realistic generalized smoothness model and aligning analysis with actual implementations—no

single work can exhaust the subject. The field remains open, with many fruitful directions left to pursue.